CANADIAN TECHNICAL REPORT OF HYDROGRAPHY AND OCEAN SCIENCES # 124

1990

# THE PULP MILL POLLUTION PROBLEM IN NEROUTSOS INLET, B.C.

by

D. J. Stucchi

Institute of Ocean Sciences
9860 West Saanich Rd.
Sidney, B.C.
V8L 4B2

Fisheries       Pêches
and Oceans      et Océans

Canada

# Canadian Technical Report of
# Hydrography and Ocean Sciences

These reports contain scientific and technical information of a type that represents a contribution to existing knowledge but which is not normally found in the primary literature. The subject matter is generally related to programs and interests of the Ocean Science and Surveys (OSS) sector of the Department of Fisheries and Oceans.

Technical Reports may be cited as full publications. The correct citation appears above the abstract of each report. Each report will be abstracted in Aquatic Sciences and Fisheries Abstracts. Reports are also listed in the Department's annual index to scientific and technical publications.

Technical Reports are produced regionally but are numbered and indexed nationally. Requests for individual reports will be fulfilled by the issuing establishment listed on the front cover and title page. Out of stock reports will be supplied for a fee by commercial agents.

Regional and headquarters establishments of Ocean Science and Surveys ceased publication of their various report series as of December 1981. A complete listing of these publications and the last number issued under each title are published in the *Canadian Journal of Fisheries and Aquatic Sciences*, Volume 38: Index to Publications 1981. The current series began with Report Number 1 in January 1982.


# Rapport technique canadien
# sur l'hydrographie et les sciences océaniques

Ces rapports contiennent des renseignements scientifiques et techniques qui constituent une contribution aux connaissances actuelles mais que l'on ne trouve pas normalement dans les revues scientifiques. Le sujet est généralement rattaché aux programmes et intérêts du service des Sciences et Levés océaniques (SLO) du ministère des Pêches et des Océans.

Les rapports techniques peuvent être considérés comme des publications à part entière. Le titre exact figure au-dessus du résumé du chaque rapport. Les résumés des rapports seront publiés dans la revue Résumés des sciences aquatiques et halieutiques et les titres figureront dans l'index annuel des publications scientifiques et techniques du Ministère.

Les rapports techniques sont produits à l'échelon régional mais sont numérotés et placés dans l'index à l'échelon national. Les demandes de rapports seront satisfaites par l'établissement auteur dont le nom figure sur la couverture et la page de titre. Les rapports épuisés seront fournis contre rétribution par des agents commerciaux.

Les établissements des Sciences et Levés océaniques dans les régions et à l'administration centrale ont cessé de publier leurs diverses séries de rapports depuis décembre 1981. Vous trouverez dans l'index des publications du volume 38 du *Journal canadien des sciences halieutiques et aquatiques*, la liste de ces publications ainsi que le dernier numéro paru dans chaque catégorie. La nouvelle série a commencé avec la publication du Rapport n° 1 en janvier 1982.

Canadian Technical Report of
Hydrography and Ocean Sciences No. 124

1990

# THE PULP MILL POLLUTION PROBLEM

# IN NEROUTSOS INLET, B. C.

by

D. J. Stucchi

Institute of Ocean Sciences
9860 West Saanich Rd.,
Sidney, B. C.
V8L 4B2

## CONTENTS

## ABSTRACT

Stucchi, D.J. 1990. The Pulp Mill Pollution Problem in Neroutsos Inlet, B.C.
Can. Tech. Rep. Hydrogr. Ocean Sci. 124: 48p.

Oceanographic and water quality data collected in Neroutsos Inlet by the
Institute of Ocean Sciences and monitoring data collected in 1986 and 1987 by
the Western Pulp Limited Partnership pulp mill staff are presented and
examined. The most severe depressions of dissolved oxygen caused by the high
BOD effluent of the mill occur from the mill site to the head of the fjord.
In this region oxygen levels are, on average, below 4 ppm at the two stations
nearest the inlet head. At the outermost station, average oxygen levels are
depressed by 0.2 ppm below the background level of 7.2 ppm. The general
circulation in the inlet consists of an outflow surface layer (0 to 5 m) with
inflow below. This circulation pattern is driven by the local winds, which
are predominantly down-inlet, but the sense of the circulation is also
consistent with classical estuarine flow. An examination of the sources and
sinks for oxygen in this fjord has revealed that the advective flux of oxygen
is the dominant source, but none of the sources and sinks could be accurately
quantified. A simple box model of the fjord, incorporating the principal
sources and sinks of oxygen, was used to explore the effects of flushing times
and BOD reaction constants on the oxygen deficit in the fjord.

Key words: pulp mill pollution, fjord circulation, Neroutsos Inlet B.C.

## RÉSUMÉ

Stucchi, D.J. 1990. The Pulp Mill Pollution Problem in Neroutsos Inlet, B.C.
Can. Tech. Rep. Hydrogr. Ocean Sci. 124: 48p.

On présente et on examine les données océanographiques et les données sur la
qualité de l'eau recueillies à Neroutsos Inlet par l'Institut des sciences de
la mer ainsi que les données de surveillance recueillies en 1986 et en 1987
par le personnel de l'usine de pâte à papier de la société en commandite
Western Pulp. Les baisses les plus graves d'oxygène dissous causées par
l'effluent à demande biologique en oxygène élévé de l'usine sont observées à
partir des environs immédiats de l'usine jusqu'à l'extrémité amont du fjord.
Dans cette région, les tenures en oxygène sont, en moyenne, inférieures à 4
ppm aux deux stations les plus proches du fond de l'inlet. A la station la
plus à l'extérieur, les teneurs moyennes en oxygène accusent une baisse de 0,2
ppm au-dessous de la concentration de fond de 7,2 ppm. La circulation
générale dans l'inlet est faite d'une couche superficielle formée par le débit
sortant (0 à 5 m), le débit entrant se trouvant au-dessous. Ce modèle de
circulation est régi par les vents locaux qui soufflent surtout en direction
de l'ouverture de l'inlet, mais le sens de la circulation est également
fonction du débit estuarien ordinaire. L'examen des sources et des puits de
ce fjord quant aux teneurs en oxygène a révélé que le flux d'advection de
l'oxygène était la pricipale source, mais qu'acune des sources et des puits ne
pouvait être quantifié avec exactitude. Un modèle de fjord en forme de simple
boîte reproduisant les principales sources est les principaux puits d'oxygène
a été employé pour étudier les effets des périodes de chasse d'eau et les

constantes reliées à la réaction de la demande biologique en oxygène sur le déficit en oxygène dans le fjord.

Mots clés: pollution de l'industrie des pâtes et papier, circulation dans ce fjord, Neroutsos Inlet, C.-B.

# I INTRODUCTION

## Background

Neroutsos Inlet is part of the Quatsino Sound group of inlets located on the northwest end of Vancouver Island (Fig. 1). It has a length of 24 km from the head to Cross Is., an average width of approximately 1.5 km, and a maximum depth of 197 m. The inlet has a deep sill (120 m) at its mouth, near Cross Island, but 34 km seaward, outside the mouth of Quatsino Sound, in the Pacific Ocean there is a shallower sill of 78 m (Fig. 2).

Port Alice, situated on the east side of the inlet 5 km from the head, is the location of a sulfite pulp mill built in 1917 and presently owned by Western Pulp Limited Partnership (WPLP). The impact of effluent discharge from the pulp mill on water quality in Neroutsos Inlet has been a long-standing concern that has lead to a number of environmental studies and pollution abatement measures (Tokar et al 1982, Cross and Ellis 1981). The reduction in the dissolved oxygen (DO) content of the surface waters by the pulp mill effluent is the principal environmental concern.

Over the years production has increased, product range expanded and pollution control measures undertaken. The most recent modification was the installation of clarifier (August 1985) to remove solids from the effluent, and the discharge of the clarified effluent through a multi-port diffuser. In spite of the increased pollution abatement equipment and procedures installed, low DO levels have continued to occur with increasing severity. The potentially serious effects that these low DO events could have on the seaward migration of juvenile salmon and on the returning adults prompted the call for a study of the circulation in Neroutsos Inlet and of the causes of these recurrent low DO events.

In Section II of this report, the temporal and spatial character of the DO field will be described using relevant data collected in the IOS study, and those monitoring data collected by the mill personnel. The circulation and anemometer data gathered during the IOS study will be presented and examined in section III. Section IV contains an examination of the sources and sinks of DO in the inlet. In section V a simple box model is formulated using the results from the previous section. Section VI provides a summary and the conclusions reached, while Section VII provides recommendations for further studies needed to resolve the oxygen deficit problem in Neroutsos Inlet.
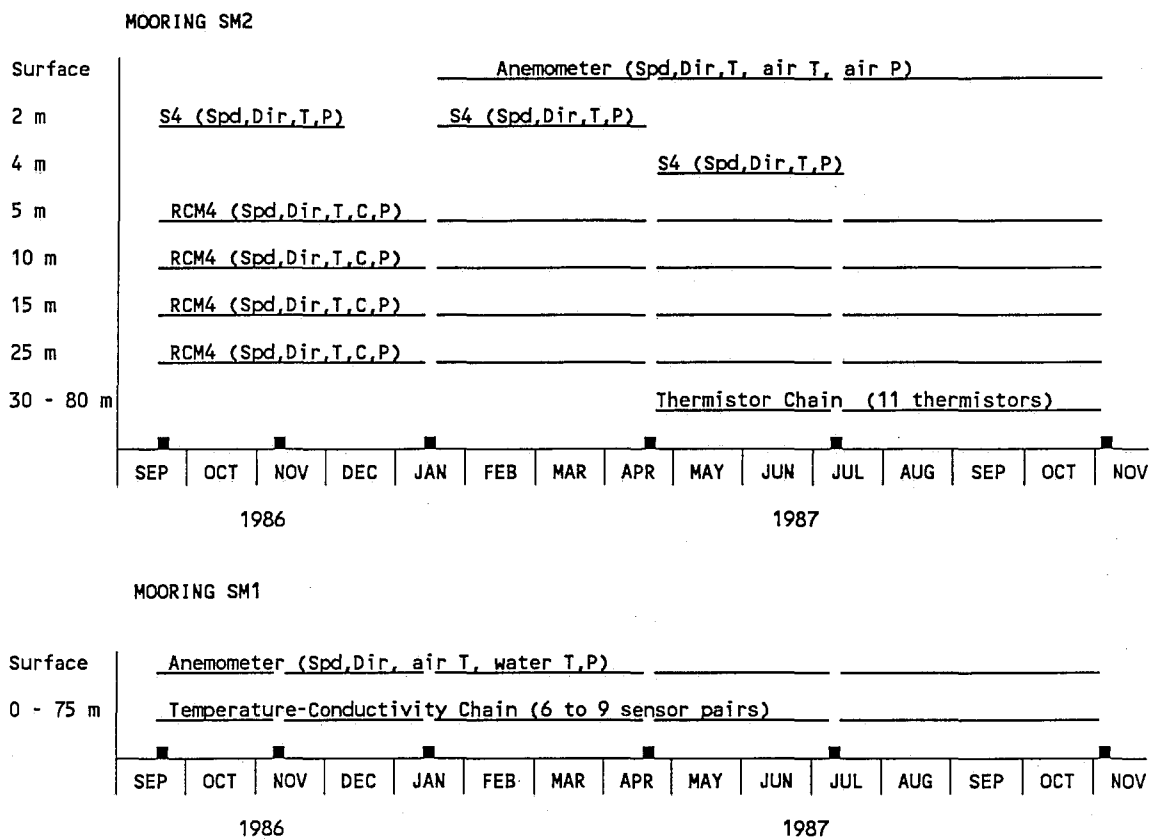
Data

There are two sets of data used in this report. The first comprises the water quality monitoring data and effluent data collected by WPLP mill operators and the second is the oceanographic and meteorological data collected by IOS.

The water quality monitoring data consists of measurements of temperature, salinity, and concentrations of dissolved oxygen (DO) and spent sulfite liquor (SSL) at discrete depths of 0, 2, 4, 6, 10, 15, 20, and 25 m (SSL measured only to 10 m). These measurements are obtained mainly at the mid-channel stations #2, #5, #8, #14, and #20 (Fig. 1). The sampling frequency is variable but generally the stations are occupied 3 times per week. Salinity measurements were determined by silver nitrate titration, and temperature data were obtained from the sensor on the Yellow Springs Instruments (YSI) DO probe. After August 1986 water temperature and salinity have been measured with an internally recording Applied Microsystems Ltd. STD-12 profiler. DO measurement were obtained with a YSI polarographic DO probe. The concentration of SSL in the water samples collected was determined using the standardized Pearl-Benson or nitroso method (Barnes et al 1963).

When the mill is in production, the effluent discharged through the diffuser is sampled daily for total flow, BOD(5), (Biochemical Oxygen Demand at 5 days) and SSL concentration. Product grade and net production information are also recorded daily. The operators also maintain a weather station at the mill site, at which precipitation, maximum and minimum air temperatures, and cloud cover are recorded daily. Data on water quality, effluent, weather and mill production are available from the mill operators for the years 1984 through 1988.

The data collected by IOS is of two types: moored instrument data and synoptic data collected during cruises in Neroutsos Inlet. The observation program began in September, 1986 with the deployment of two surface moorings, (SM1 and SM2) and two bottom mounted pressure gauge sites (Fig. 1), and ended in November 1987, at which time all the instrumentation was recovered. The moorings were serviced every 3 to 4 months over this period, with a total of six cruises in the inlet. Table 1 summarizes the type, location and time history of the moored instrument data collect in Neroutsos Inlet.

Table 1. Summary of the type (RCM4 = Aanderaa current meter, S4 = Interocean vector averaging current meter), location and time history of moored instrument data collected in Neroutsos Inlet by the Institute of Ocean Sciences. The solid squares on the time axes indicate the time of the cruises to Neroutsos Inlet.


MOORING SM2

| Surface | | | Anemometer (Spd,Dir,T, air T, air P) | | | |
|---|---|---|---|---|---|---|
| 2 m | S4 (Spd,Dir,T,P) | | S4 (Spd,Dir,T,P) | | | |
| 4 m | | | | S4 (Spd,Dir,T,P) | | |
| 5 m | RCM4 (Spd,Dir,T,C,P) | | | | | |
| 10 m | RCM4 (Spd,Dir,T,C,P) | | | | | |
| 15 m | RCM4 (Spd,Dir,T,C,P) | | | | | |
| 25 m | RCM4 (Spd,Dir,T,C,P) | | | | | |
| 30 - 80 m | | | | Thermistor Chain (11 thermistors) | | |

| SEP | OCT | NOV | DEC | JAN | FEB | MAR | APR | MAY | JUN | JUL | AUG | SEP | OCT | NOV |

1986                                           1987


MOORING SM1

| Surface | Anemometer (Spd,Dir, air T, water T,P) | | |
|---|---|---|---|
| 0 - 75 m | Temperature-Conductivity Chain (6 to 9 sensor pairs) | | |

| SEP | OCT | NOV | DEC | JAN | FEB | MAR | APR | MAY | JUN | JUL | AUG | SEP | OCT | NOV |

1986                                           1987


Both surface moorings were taut line moorings, having a 2.4 m diameter toroidal surface buoy as the main source of buoyancy. The surface buoys were both instrumented with Aanderaa weather stations capable of sampling wind speed and direction, wind gusts, air pressure, air and surface water temperature. The anemometer sensors were positioned 3.3 m above the water surface, and the surface temperature sensor was placed at a depth of 25 cm. The data were internally recorded every 30 minutes. The southern mooring (SM1) initially deployed off Thurburn Bay was redeployed 2 km to the northwest in November, 1986 to the position indicated in Fig. 1. The first deployment of surface mooring SM2, near Buccholtz Rock, was without a weather station.

Mooring SM2 was instrumented with five current meters, positioned at depths of 2, 5, 10, 15 and 25 m. The shallowest meter was an Interocean S4 vector averaging current meter, and Aanderaa RCM4's fitted with temperature and conductivity sensors were used at the remaining depths. The Interocean S4

recorded integrated velocity for 2 minutes every 30 minutes, while the RCM4's sampled every 30 minutes. The S4 current meter was positioned at a depth of 4 m from April to July, 1987, and not used subsequently. Below the current meters, a 50 m Aanderaa thermistor chain and data logger were attached to the mooring. The thermistors were spaced 5 m apart from 30 to 80 m, and sampled every 60 minutes.

The southern mooring, SM1 was instrumented with an Applied Microsystems Ltd. temperature-conductivity chain and data logger. Depending on the time of the deployment, 6 to 8 canisters containing temperature and conductivity sensors were positioned with increasing separation from 2.75 to 75 m in depth. The sampling interval used was either 30 or 60 minutes.

The bottom mounted pressure gauges deployed were Applied Microsystem Ltd. model 750A or TG-12A, and Aanderaa model TG-3A. The gauges were deployed by divers in water depths less than 10 m. The sampling interval was 30 minutes, with integration time varying from 28 to 900 seconds depending on the model used. The gauges were serviced only once, in July 1987.

During the six cruises, profiles of temperature and salinity were obtained using Guildline Instruments Ltd. CTD (conductivity, temperature and depth) probes, and on the last cruise (Nov. 1987) a CTD probe fitted with a polarographic DO sensor was used to obtain a vertical profile of DO. Classical bottle casts using 1.7 litre Niskin bottles obtained water samples for DO determinations using the Winkler method. These CTD and DO data were collected at 13 station located in Quatsino Sound and Neroutsos Inlet (Fig. 1). In addition to the regular sampling stations 12 to 24 hour time series of CTD profiles, taken every 30 minutes, were obtained as close as practical to moorings SM1 and SM2 before and after deployment. The CTD data were later used to calibrate the temperature and conductivity sensors on the Aanderaa RCM4's and the Applied Microsystems Ltd. temperature-conductivity chain.

## II THE LOW DO PROBLEM

The principal concern, though not the only one, regarding the discharge of pulp mill effluent into the surface waters of Neroutsos Inlet is the severe reduction in the DO content that results. Adequate DO levels are necessary for the survival and growth of healthy fish populations. Davis (1975) in his review of the oxygen requirements of aquatic life has stated that low oxygen levels adversely affect growth, and have marked effects on the physiological, biochemical and behavioral processes in fish. He developed oxygen criteria for various fish populations and from these he devised three levels of protection. Level A represents ideal conditions and assures a high degree of safety. Level B represents the level where the fish start to exhibit some

symptoms of oxygen distress. At level C large portions of the fish population are affected, and deleterious effects may be serious. He defines limiting values for anadromous marine species, including salmonids, to be 9.0, 6.5 and 4.0 ppm $O_2$ for levels A, B, and C respectively.

The toxicity of the effluent, and the dark humic staining of the fjord surface waters are also of concern but these are overshadowed by the reduction in DO levels. The deleterious effects of extremely low oxygen levels may be exacerbated by toxic compounds introduced by the effluent. In this section monitoring data collected by the mill environmental staff from 1986 to 1988, and synoptic data obtained by IOS will be presented and used to describe spatial and temporal extent of the low DO problem.

Before these data are examined it is useful to present data collected outside of Neroutsos Inlet, and therefore not subject to the influence of the pulp mill. Such "background" data have been and are still being collected, by the environmental staff of the Island Copper Mine, at station D in Quatsino Sound, near IOS station Q4 (Fig. 1). The time series of monthly DO measurements for this Quatsino Sound station began in 1971, and was made available by Mr. R. Hillis of Island Copper Mine (unpublished data). The calculation of the monthly DO means (Table 2) did not use data obtained before 1978, since in the early 1970's Tokar et al (1982) reported that the mill was discharging large daily BOD(5) loads (upto $227 \times 10^3$ kg $O_2$) and DO levels were therefore being affected in Quatsino Sound. The installation of a liquor incineration system in 1977 reduced BOD(5) discharge by about 70%, and DO levels subsequently improved (Tokar et al 1982).

Table 2.  Monthly averaged DO levels at 0, 5 and 30 m depth, (1978 through 1985) taken in Quatsino Sound near IOS station Q4.

| Month | Dissolved Oxygen (ppm) | | | |
|---|---|---|---|---|
|  | 0 m | 5 m | 30 m | 30 m Avg. |
| January | 7.69 | 7.45 | 7.76 | 7.60 |
| February | 7.99 | 7.79 | 7.80 | 7.82 |
| March | 8.62 | 8.28 | 8.41 | 8.36 |
| April | 8.26 | 8.00 | 8.00 | 8.03 |
| May | 8.26 | 8.23 | 7.47 | 7.91 |
| June | 7.62 | 7.51 | 6.14 | 6.95 |
| July | 8.16 | 7.56 | 6.20 | 7.04 |
| August | 7.87 | 7.37 | 5.51 | 6.64 |
| September | 7.53 | 7.13 | 6.13 | 6.75 |
| October | 6.98 | 6.30 | 6.07 | 6.26 |
| November | 6.84 | 6.20 | 6.43 | 6.35 |
| December | 6.70 | 6.67 | 7.09 | 6.84 |
| 12 month Avg. | 7.71 | 7.37 | 6.92 | 7.21 |

Protection level A oxygen values are rarely achieved in Quatsino Sound (station Q4), but level B values and higher are almost always present in the surface waters and at 5 m depth.  At 30 m, level B values are not achieved during the summer and fall months but even then DO values are still well above level C values (4 ppm) and usually above 5 ppm.  The annual 0 to 30 m depth averaged DO value for the Quatsino Sound data (Table 2) is 7.2 ($\pm$0.7) ppm. The natural seasonal variation in the background DO levels should be taken into consideration when implementing the protection level criteria for Neroutsos Inlet.

Examination of the depth-time contours of DO at two different stations offers a perspective on the temporal development of the vertical DO profile. Depth-time contours of DO at station #2 (Fig. 3) reveal that the low DO conditions - well below protection level C for salmonids - span the depth range of the measurements (0 to 25 m) and can occur for periods as long as 30 to 40 days.  Shorter period fluctuations of 15 to 25 days are also evident. Often the DO content is less than 1 ppm; DO levels of 5 ppm and higher are seldom found except at the surface.  At station #14 (Fig. 4) the general DO level is considerably higher; extremely low DO conditions are limited in vertical extent and of considerably shorter duration.

Axial cross sections of DO offer a two-dimensional (X-Z) perspective. DO profiles taken during the IOS cruises and contoured in the X-Z plane (Figs. 5 and 6) clearly show that the zone of most severe impact extends from station

#8 to the head of the fjord, but that depressed DO levels can occur as far down inlet as station N18. The vertical structure is often complicated by the interleaving of layers of low and high DO water, and horizontally, "pockets" of low DO water are also evident. The survey of July 5, 1987 is noteworthy because it shows severe DO depletion from station #11 to the head, with DO absent, or not measurable, in the depth range from 2 to 15 m. Except for a thin surface layer DO levels were less than 1 ppm to a depth of 25 m. Up-inlet from station #11 (6.5 km from the head) DO levels are well below protection level C values. Isolated, thin "pockets" of low DO water were also observed, one extending from station #14 to #20 during the same survey. In contrast, the survey of April 15, 1987 reveals conditions of relatively high DO levels in the fjord, nevertheless the impact of the effluent is evident from station #8 to the head, where once again DO values are at or below those of protection level C. At this time of year such low values are of particular concern because juvenile salmon migration from the streams to the fjord is underway (Poulin and Oguss 1982).

An alternate approach to the characterization of the DO field in Neroutsos Inlet is offered by EOF (Empirical Orthogonal Function) analysis. In EOF analysis a set of correlated data - such as the present DO time series from the different depths and stations - is represented by eigenvectors or eigenfunctions, the corresponding eigenvalues and the time dependant amplitude functions. The eigenfunctions represent the spatial characters of the different modes and the corresponding eigenvalue indicates the amount of variance contained in the particular mode. The temporal character of the particular mode is given by the corresponding time amplitude function. Usually only a few modes are needed to describe most of the variance, and they each may have a physical interpretation.

The mathematics underlying the EOF calculation are described by Kutzbach (1967). Simply stated, the analysis consists of finding the eigenvalues and eigenvectors of the cross correlation matrix computed from the observation vectors (time series of DO at different depths and stations). Such analysis was undertaken on the DO time series from the eight depths (0, 2, 4, 6, 10, 15, 20, 25 m) sampled at the five stations #2, #5, #8, #14 and #20 - a total of 40 time series or observation vectors. The vectors were normalized - to zero mean and unit variance - so that each observation point or location was of equal importance in the EOF representation of the DO field, and a cross correlation matrix of dimensions 40 x 40 was computed. The period from October 17, 1986 to June 29, 1987 (256 days) was analyzed.

The mean DO field shown in Table 3 confirms the earlier assessment, namely that the most severe DO depression occurs from station #8 to the head,

with station #2 showing the lowest mean DO levels ( < 3 ppm from 6 to 20 m). Station #2 and #5 are on average well below protection level C in DO content (except for the surface values). The surface is high in DO ( > 6 ppm ) at all stations. From station #8 to the head, subsurface DO values are generally below 5 ppm, while at stations #14 and #20 DO values are greater than 5 ppm DO. DO content at Station #20, which is the least affected by the mill effluent approaches background values (Table 2), and is above protection level B.

Table 3. The mean DO (ppm) field at stations #2, #5, #8, #14, and #20 at depths of 0, 2, 4, 6, 10, 15, 20 and 25 m.

| DEPTH | STATION | | | | |
|---|---|---|---|---|---|
| (m) | #2 | #5 | #8 | #14 | #20 |
| 0 | 6.72 | 6.37 | 6.18 | 6.13 | 6.98 |
| 2 | 3.46 | 3.58 | 4.32 | 5.78 | 7.02 |
| 4 | 3.00 | 3.31 | 3.94 | 5.77 | 6.99 |
| 6 | 2.78 | 2.95 | 3.73 | 5.86 | 7.00 |
| 10 | 2.70 | 3.00 | 3.92 | 6.05 | 6.99 |
| 15 | 2.70 | 3.25 | 4.12 | 5.94 | 7.05 |
| 20 | 2.79 | 3.35 | 4.18 | 6.03 | 6.99 |
| 25 | 3.21 | 3.87 | 4.52 | 6.27 | 7.08 |

The DO variance field (Table 4) shows that the variance is smallest at stations #14 and #20, and generally decreases from the surface to 25 m. The highest variance is observed at stations #2, #5, and #8 - the stations that are most affected by the mill.

Table 4.  The variance of the DO field at stations #2, #5, #8, #14, and #20 at depths of 0, 2, 4, 6, 10, 15, 20 and 25 m.

| DEPTH (m) | STATION | | | | |
|---|---|---|---|---|---|
| | #2 | #5 | #8 | #14 | #20 |
| 0 | 3.29 | 3.07 | 3.29 | 3.71 | 1.90 |
| 2 | 3.97 | 3.81 | 3.98 | 3.40 | 1.36 |
| 4 | 3.85 | 3.88 | 3.94 | 3.17 | 1.14 |
| 6 | 3.81 | 3.93 | 4.16 | 2.53 | 0.67 |
| 10 | 3.95 | 4.70 | 3.99 | 2.02 | 0.59 |
| 15 | 3.59 | 4.53 | 4.03 | 2.68 | 0.54 |
| 20 | 3.05 | 3.84 | 3.57 | 2.23 | 0.84 |
| 25 | 2.24 | 1.87 | 2.70 | 1.26 | 0.54 |

The first 3 EOF modes account for almost 77% of the total variance; the first mode alone has an eigenvalue of 19.8 and accounts for 49.6% of the total variance, the second mode has an eigenvalue of 6.3 (15.8% of total variance), and the third mode has an eigenvalue of 4.6 (11.4% of total variance). The fourth, fifth and sixth modes account for another 10.6% of the total variance. Only the first 3 modes will be presented and discussed as they account for the bulk of the total variance.

Table 5.  The eigenfunction for the first EOF mode, and in parentheses, the percentage of variance from the individual locations in this mode.

| DEPTH (m) | STATION | | | | |
|---|---|---|---|---|---|
| | #2 | #5 | #8 | #14 | #20 |
| 0 | -0.11 (24) | -0.11 (24) | -0.15 (45) | -0.17 (57) | -0.15 (45) |
| 2 | -0.16 (51) | -0.17 (57) | -0.18 (64) | -0.16 (51) | -0.12 (29) |
| 4 | -0.18 (64) | -0.19 (72) | -0.19 (72) | -0.15 (45) | -0.13 (34) |
| 6 | -0.20 (79) | -0.21 (88) | -0.20 (79) | -0.14 (39) | -0.11 (24) |
| 10 | -0.20 (79) | -0.20 (79) | -0.17 (57) | -0.15 (45) | -0.11 (24) |
| 15 | -0.19 (72) | -0.18 (64) | -0.17 (57) | -0.14 (39) | -0.11 (24) |
| 20 | -0.18 (64) | -0.18 (64) | -0.17 (57) | -0.15 (45) | -0.12 (29) |
| 25 | -0.09 (16) | -0.12 (29) | -0.14 (39) | -0.14 (39) | -0.12 (29) |

The eigenfunction for the first mode (Table 5) shows an in-phase response at all stations, with the strongest response characterizing the most affected stations and depths i.e., stations #2, #5, and #8 at depths below the surface and above 25 m.  The response is generally weakest at or near the

surface and at depth at the outermost stations (#14 and #20), which is indicative of other processes contributing to the DO fluctuations at these locations. From an examination of the variance associated with this first mode from the individual locations (Table 5) it is apparent that - at those stations where the DO depressions are largest - 60 to 88% of the variance from the individual time series is associated with this mode. At the surface and at the outermost stations only 24 to 57% of the variance from the individual locations is accounted for by this mode. At 25 m, 16 to 39% of the variance from these locations is contributed to this mode. The mode probably represents the basic impact of the effluent on the DO levels in the fjord. The impact is felt to a greater or lesser degree at all stations and the response is in phase at all stations.

The eigenfunction of the second EOF mode (15.8% of the total variance) has a zero crossing, in its vertical structure, between 6 and 10 m at all stations (Table 6). The DO fluctuations in the top layer are therefore 180° out of phase with those in the deeper layer. As such this mode may represent the baroclinic response of the fjord - a similar two-layer structure can also be seen in the vertical current structure (Section III). The horizontal structure within the surface layer is relatively uniform. Most of the variance in this mode originates from 0 to 2 m and from 20 to 25 m in depth.

Table 6. The eigenfunction for the second EOF mode, and in parentheses, the percentage of variance from the individual locations in this mode.

| DEPTH (m) | STATION #2 | #5 | #8 | #14 | #20 |
|---|---|---|---|---|---|
| 0 | 0.25 (39) | 0.25 (39) | 0.23 (33) | 0.21 (28) | 0.18 (20) |
| 2 | 0.18 (20) | 0.18 (20) | 0.11 ( 8) | 0.22 (31) | 0.21 (28) |
| 4 | 0.13 (11) | 0.13 (11) | 0.05 ( 2) | 0.16 (16) | 0.15 (14) |
| 6 | 0.05 ( 2) | 0.00 ( 0) | -0.01 ( 0) | 0.09 ( 5) | 0.08 ( 4) |
| 10 | -0.05 ( 2) | -0.13 (11) | -0.20 (25) | -0.07 ( 3) | -0.05 ( 2) |
| 15 | -0.09 ( 5) | -0.18 (20) | -0.19 (23) | -0.12 ( 9) | -0.07 ( 3) |
| 20 | -0.14 (12) | -0.19 (23) | -0.21 (28) | -0.14 (12) | -0.12 ( 9) |
| 25 | -0.22 (31) | -0.24 (36) | -0.21 (28) | -0.16 (16) | -0.06 ( 2) |

The eigenfunction from the third EOF mode (11.4% of the total variance) has a horizontal zero-crossing at station #8, with the strongest response subsurface at station #20 (Table 7). The DO fluctuations from stations #8, #5 and #2 are generally 180° out of phase with those at stations #14 and #20. Most (70%) of the variance in this third mode comes from depths below 2 m at stations #14 and #20. This mode may represent the background fluctuations in

the DO field, as the response is largest at the outermost stations where the impact of the effluent is lowest.

Table 7.  The eigenfunction for the third EOF mode, and in parentheses, the percentage of variance from the individual locations in this mode.

| DEPTH | STATION | | | | |
|---|---|---|---|---|---|
| (m) | #2 | #5 | #8 | #14 | #20 |
| 0 | -0.01 ( 0) | 0.05 ( 1) | 0.07 ( 2) | 0.04 ( 1) | -0.01 ( 0) |
| 2 | 0.16 (12) | 0.15 (10) | 0.15 (10) | -0.04 ( 1) | -0.09 ( 4) |
| 4 | 0.13 ( 8) | 0.09 ( 4) | 0.08 ( 3) | -0.12 ( 7) | -0.20 (18) |
| 6 | 0.10 ( 5) | 0.06 ( 2) | 0.01 ( 0) | -0.21 (20) | -0.31 (44) |
| 10 | 0.11 ( 6) | 0.06 ( 2) | -0.02 ( 0) | -0.23 (24) | -0.31 (44) |
| 15 | 0.13 ( 8) | 0.06 ( 2) | -0.02 ( 0) | -0.22 (22) | -0.33 (50) |
| 20 | 0.17 (13) | 0.09 ( 4) | 0.07 ( 2) | -0.14 ( 9) | -0.29 (38) |
| 25 | 0.23 (24) | 0.15 (10) | 0.12 ( 7) | -0.11 ( 6) | -0.28 (36) |

## III NEAR SURFACE CIRCULATION

In this section the near-surface circulation, as inferred from the current meter and anemometer data collected at mooring SM2, will be presented and analyzed.  However, before any of the data are presented a major deficiency in data quality will be discussed.  It became evident that the currents measured below the surface buoy at SM2 were much too large to be realistic;  the buoy motion and surface wave action were causing the "pumping" of the Savonius rotors of the Aanderaa current meters and thus speeds obtained from these meters to be overestimated.  A vector-averaging current meter (Interocean S4) was initially positioned at 2 m depth, but on the third deployment is was placed less than 0.5 m from the rotor of the Aanderaa RCM4 at 5 m depth.  Comparison of the speed data from these two closely spaced instruments showed that those from the Aanderaa were as much as two times larger than those measured with the vector averaging meter.  The direction information is not seriously influenced, as the principal axis of the variance is still aligned with that of the fjord, although there is considerably more noise in the Aanderaa data than in those from the Interocean S4. Nevertheless, in spite of the above mentioned deficiency, important information can be obtained about the near-surface circulation in this fjord from the vertical structure of and fluctuations in the data.

The current data collected at mooring SM2 have been low-pass filtered with a cosine-Lanczos filter (half-power point at 40 hrs) and then transformed

to flow directed into (-ve) or out of (+ve) the fjord (Fig. 7). For the period (September 1986 to April 1987), the general circulation pattern is one of surface outflow (0 to 5 m) and inflow at depths of 10 and 15 m. The first zero-crossing in the vertical current structure occurs at about 5 m depth. The flow pattern below 5 m depth is on average towards the southeast (up-inlet) for the entire (400 day) length of the time series. (It should be noted that surface measurements (2 m) were not obtained after April, 1987). The currents appear to be coherent in the vertical, although the 25 m currents appear to be notably less coherent (Table 8). The time scale of the fluctuations appears to cover a wide range from 2 to 5 days and up to longer periods of 20 days.

The anemometer data collected at moorings SM1 and SM2 were also low-pass filtered, and the wind velocity resolved into components along and across the fjord axis (Fig. 8). The predominant direction of the winds is to the northwest during the fall, winter and spring but during the summer they reverse direction and blow primarily up-inlet. Unfiltered wind speed are sometimes as high as 15 m s$^{-1}$, but are typically in the range 5 to 10 m s$^{-1}$. Winds measured at SM1 and SM2 are strongly coherent, and data from either location are therefore representative of the wind field in the fjord.

The winds and the currents, especially the near-surface currents, appear visually to be correlated. The sense of the general near-surface circulation described above is consistent with a wind driven response of the fjord. In winter, the down inlet winds frictionally drive a surface (2 m) outflow, below which there is a compensating inflow. The reverse occurs during the summer; the winds generally blow up the inlet (towards the southeast) and the flow below 5 m depth is down inlet. Because the current meter data and wind data appear to be correlated, the fluctuations in the combined current and wind fields will be described using EOF analysis.

The principal EOF modes of all the available low-passed current meter and anemometer data are computed for each of the four deployments of the SM2 mooring (see Table 10). The individual current and wind time series are demeaned and normalized to unit variance, and then the correlation matrix is computed. The correlation matrix (Table 8) for the second deployment of SM2 (January 19 to April 4, 1987) quantifies the visual similarity between the time series alluded to above, the other deployment have similar correlation matrices. Almost all of the variance in the current and wind fields is accounted for by the first three modes, the first two modes usually account for about 80% of the total variance (Table 9).

Table 8.   Correlation matrix for the low-passed, along channel current and wind data from the second deployment (January 19 to April 4, 1987) of mooring SM2.

|  | Wind | Current | | | | |
|---|---|---|---|---|---|---|
|  |  | 2 m | 5 m | 10 m | 15 m | 25 m |
| Wind | 1.0 | 0.8 | 0.3 | -0.5 | -0.6 | -0.1 |
| Current (2 m) | 0.8 | 1.0 | 0.3 | -0.5 | -0.6 | -0.1 |
| Current (5 m) | 0.3 | 0.3 | 1.0 | 0.1 | -0.3 | -0.1 |
| Current (10 m) | -0.5 | -0.5 | 0.1 | 1.0 | 0.7 | -0.2 |
| Current (15 m) | -0.6 | -0.6 | -0.3 | 0.7 | 1.0 | 0.2 |
| Current (25 m) | -0.1 | -0.1 | -0.1 | -0.2 | 0.2 | 1.0 |

Table 9.   Eigenvalues and % variance accounted for in the first three EOF modes of the current and wind data from the four deployments of mooring SM2.

| Deployment # (dates) | Eigenvalue (% variance) | | |
|---|---|---|---|
|  | Mode 1 | Mode 2 | Mode 3 |
| 1 (Sep. 20 - Nov. 26, 1986) | 2.54 (42.3) | 2.16 (36.1) | 0.71 (11.9) |
| 2 (Jan. 19 - Apr.  4, 1987) | 2.87 (47.8) | 1.27 (21.1) | 0.93 (15.5) |
| 3 (Apr. 21 - Jul.  5, 1987) | 3.11 (51.9) | 1.79 (29.9) | 0.60 (10.0) |
| 4 (Jul. 11 - Oct. 25, 1987) | 2.26 (45.3) | 1.89 (37.8) | 0.45 ( 9.1) |

The eigenfunctions for the first three modes and the percentage of variance from an individual location explained by that mode are tabulated in Table 10.  During the second and third deployments the first EOF mode, which accounts for about 50% of the total variance, is a wind driven mode as over 70% of the wind variance and over 50% of the current meter variance are tied up in this mode.   The mode 1 eigenfunctions for both these deployments indicate that the near surface current response is in phase with the winds. Both eigenfunctions have a zero-crossing between 5 and 10 m, and possible a second zero-crossing at 25 m for the second deployment.  In addition to the strong response of the currents at 2 m to the wind, the currents at 15 m depth also show a strong response to the wind forcing.  The first EOF mode for the fourth deployment has a similar structure but the amount of wind variance in this mode is less than 50% and the first zero-crossing is shallower than 5 m. However the currents at 10, 15 and 25 m depth respond strongly to this mode,

The wind driven mode for the first deployment is the second EOF mode and it has its zero-crossing between 2 and 5 m.

The first EOF mode of deployment #1 and the second EOF mode for deployment #4 contain about 25% of the wind variance but the main contribution is from the currents in the top 10 m. The variance in the second EOF modes of the second and third deployments originates from the currents at 4 to 10 m in depth, with virtually no contribution from the wind. The vertical structure of these modes is variable but they are generally characterized by a zero-crossing deeper in the water column between 15 and 25 m or deeper. An explanation for these secondary modes is not clear.

The third EOF modes for all four deployments usually accounts for only 10 to 15% of the total variance, and the response is erratic. On deployments #3 this third EOF represents primarily the variance contained in the currents at 25 m. No explanation for this third EOF mode is offered.

Table 10.  Eigenfunctions and the percentage of variance from the individual time series in the first three EOF modes of the wind and current data from the four deployments of mooring SM2.

| Deployment # (dates) | Location | Eigenfunction (% variance) | | |
|---|---|---|---|---|
| | | Mode 1 | Mode 2 | Mode 3 |
| 1 | Wind | 0.31 (24) | -0.50 (54) | 0.24 ( 4) |
| | Cur  2 m | 0.45 (51) | -0.18 ( 7) | 0.69 (34) |
| Sep. 20, 1986 | Cur  5 m | 0.58 (85) | 0.12 ( 3) | -0.22 ( 3) |
| to | Cur 10 m | 0.50 (64) | 0.35 (27) | -0.29 ( 6) |
| Nov. 26, 1986 | Cur 15 m | 0.21 (11) | 0.58 (73) | 0.18 ( 2) |
| | Cur 25 m | -0.27 (19) | 0.49 (52) | 0.55 (22) |
| 2 | Wind | -0.51 (75) | -0.06 ( 0) | 0.00 ( 0) |
| | Cur  2 m | -0.51 (75) | -0.11 ( 2) | -0.10 ( 1) |
| Jan. 19, 1987 | Cur  5 m | -0.21 (13) | -0.56 (40) | -0.65 (39) |
| to | Cur 10 m | 0.43 (53) | -0.51 (33) | -0.16 ( 2) |
| Apr.  4, 1987 | Cur 15 m | 0.49 (69) | 0.00 ( 0) | -0.20 ( 4) |
| | Cur 25 m | 0.03 ( 0) | 0.64 (52) | -0.71 (47) |
| 3 | Wind | 0.48 (72) | -0.14 ( 4) | -0.32 ( 6) |
| | Cur  4 m | 0.36 (40) | 0.54 (52) | -0.22 ( 3) |
| Apr. 21, 1987 | Cur  5 m | 0.31 (30) | 0.60 (65) | -0.13 ( 1) |
| to | Cur 10 m | -0.36 (40) | 0.51 (47) | 0.33 ( 7) |
| Jul.  5, 1987 | Cur 15 m | -0.49 (75) | 0.27 (13) | -0.07 ( 0) |
| | Cur 25 m | -0.42 (55) | -0.01 ( 0) | -0.85 (43) |
| 4 | Wind | 0.46 (48) | -0.37 (26) | -0.71 (23) |
| Jul. 11, 1987 | Cur  5 m | -0.08 ( 1) | -0.67 (85) | 0.48 (10) |
| to | Cur 10 m | -0.41 (38) | -0.54 (55) | -0.04 ( 0) |
| Oct. 25, 1987 | Cur 15 m | -0.59 (79) | -0.12 ( 3) | -0.52 (12) |
| | Cur 25 m | -0.52 (61) | 0.34 (22) | -0.08 ( 0) |

## IV DISSOLVED OXYGEN SOURCE AND SINK

Introduction

In this section the various terms in the DO budget of Neroutsos Inlet are estimated and examined in order to gain some insight into the magnitude and relative importance of the sources and sinks of DO, the time scales of their fluctuations, their spatial distributions, and the problems associated

with their estimation. Any progress made in identifying the dominant terms and the deficiencies in sampling strategy or procedures will help to focus future investigations, and hopefully lead to realistic estimates of the assimilative capacity of the fjord and of the degree of secondary treatment required for the satisfactory resolution of the pollution problem. The exercise of actually balancing the DO budget is not attempted for reasons that will become obvious later in this section.

If the advective-diffusive equations are integrated over a volume of the fjord defined by a distance x from the head, the breadth, and depth from the surface to the bottom, then the time rate of change of the total amount C of biodegradable organic matter in this volume is given by

$$\frac{dC}{dt} = -\int_{A_x} (u \cdot c) dA + \int_{A_x} (K_H \cdot \frac{dc}{dx}) dA - F + Q_M \tag{1}$$

where c is the concentration of organic matter, $A_x$ is the cross sectional area at x, $K_H$ is the horizontal eddy diffusivity and u is the along channel velocity component. The first two terms on the right hand side of the above equation are, respectively, the advective and diffusive fluxes of organic matter across $A_x$. The third term, F, is the rate of consumption of the organic matter (stabilization) by microorganisms and the last term is simply the rate at which the mill injects organic matter into the fjord. It is assumed that the flux of organic matter from the sediments and from the runoff to the fjord is negligible.

The water quality parameter of concern is the dissolved oxygen content and the corresponding integrated advective-diffusive equation is

$$\frac{dO}{dt} = -\int_{A_x} (u \cdot DO) dA + \int_{A_x} (K_H \cdot \frac{dDO}{dx}) dA - BOD + AIRSEA - SOD + others \tag{2}$$

where O is the total dissolved oxygen content of the volume of integration, and DO is the dissolved oxygen concentration. The first and second terms on the right hand side are, as before, the advective and diffussive fluxes. The third term, BOD, represents the rate at which oxygen is consumed by the microorganisms as they metabolize the organic matter C. The fourth term, AIRSEA, represents the air-sea exchange of oxygen, and the

fifth term is the sediment oxygen demand (SOD). The last term encompasses a number of other sources and sinks for DO, including any DO produced by photosynthesis.

Equations (1) and (2) are coupled through the BOD and organic decay (F) terms, since oxygen is consumed in direct proportion to the consumption of organic matter. The determination of the DO balance or budget is dependant on a number of different processes. The oceanography enters primarily through the advective term, while the meteorology influences the air-sea gas exchange. The biochemistry and biology are represented by the reaction which oxidizes the organic matter. The industrial process provides the primary forcing to the water quality parameters through the injection rate of the mill effluent, the effluent's organic composition and toxins. The spatial extent and the severity of DO depressions in the fjord are the results of a balance between the industrial and biochemical processes which supply and consume the organic matter, on the one hand, and the oceanographic and meteorological processes which replenish and distribute the DO, on the other.

Change in total DO content

The time derivative of the total DO content (left hand side of equation (2)) represents the net effect of all the source and sink terms in the DO budget of the fjord. Estimation of this term is pursued because the magnitude and fluctuations may provide information about the scale of the problem, and also aid in defining the relative importance of each term in the DO budget.

The change in the total DO content of Neroutsos Inlet is approximated by using the volume of integration determined by the stations and depths sampled by the mill personnel. The control volume V for this calculation extends from the head of the fjord to station #20 and from the surface to 25 m depth, and equals $4.49 \times 10^8$ m$^3$. The surface area A involved is $18.0 \times 10^6$ m$^2$. Generally this volume encompasses the impact zone of the effluent, although it is evident that at times the effects of the mill extend below 25 m (Fig. 3) and beyond station #20 (Fig. 5). Within this volume, DO is sampled at stations #2, #5, #8, #14, and #20 at depths of 0, 2, 4, 6, 10, 15, 20 and 25 m. The temporal coverage of the above stations consists of approximately 3 surveys per week from October 1986 to the present, with the exception that station #20 was often sampled only once per week in the period from October 1986 to March 1987.

Before the volume integration of DO is carried out the station data is interpolated in time to give daily values. The calculation of total DO content is performed by vertically integrating the horizontally averaged DO

data and multiplying the result by the surface area A of the control volume. The calculation is repeated for each day of data in the station DO time series to produce a daily time series of total DO content of the control volume (Fig. 9a). The daily time rate of change of DO content is then simply the first difference of the time series (Fig. 9b,c).

The total DO content varies between 1 and 4 $\times$ $10^6$ kg $O_2$. In more practical terms, the corresponding average DO concentration is 2 to 8 ppm. The summer of 1987 (July and August) had consistently low DO values 3 to 4 ppm though shorter term DO depressions are evident during the winter months. In fact, the lowest DO content was observed in January 1988 (2 ppm). The high DO content of April 1987 is attributed to the spring phytoplankton bloom (Seaconsult 1987) but the peak values observed in January 1987 are as yet unexplained. Over the 460 day span of the time series a decreasing trend in the DO is discernible.

The daily change in DO content (Fig. 9b) is by comparison a noisy times series, as is to be expected when a signal is differentiated. The daily changes in DO content are approximately as large as $\pm 600 \times 10^3$ kg $O_2$ $d^{-1}$, but are generally less than $\pm 250 \times 10^3$ kg $O_2$ $d^{-1}$. The "smoothing" effect of the weekly sampling at station #20 is evident by the near constant daily DO changes for periods of 7 days or more in the early part of 1987.

Advective Flux of Oxygen

The advective flux term for the control volume consists of the two components shown:

$$\text{Advective Flux} = -B \int_0^{25} (u \cdot DO) dz + \int_0^B \int_0^S (w \cdot DO) dxdy \qquad (3)$$

where B is the breadth of the fjord at station #20, S is the distance from the head to station #20, and w is the vertical velocity. The first term of equation (3) is the horizontal DO flux through the cross section at station #20 from the surface to 25 m, and the second is the vertical DO flux through the bottom surface of the control volume (25 m depth). The horizontal flux is estimated using the low-passed, along-channel currents from mooring SM2 (2, 5, 10, 15 and 25 m) and the daily DO data from station #20. The flux is calculated by taking the depth integral of the product of the linear profiles of current and DO, over the total number of depth intervals determined by the spacing of the current meters. The vertical DO flux is estimated by taking

the product of the horizontally averaged DO concentration at 25 m and the horizontally averaged vertical velocity. Since the vertical velocity cannot be directly measured, continuity is used to calculated the horizontally averaged vertical velocity as indicated below

$$\overline{w} \; = \; \frac{1}{A} \left[ \; B \int_{0}^{25} u \cdot dz \; \right] \tag{4}$$

where A is the area of the bottom surface (z = 25 m) of the control volume, and the quantity enclosed in the square brackets is the volume flux. The errors in the currents carry over directly to this term.

The time series of the horizontal and vertical DO fluxes (Fig. 10b and c) are almost mirror images of each other and have large opposing DO transports. The horizontal DO transport through the section at station #20 is most often a positive flux (a source of DO - transport into the control volume) while the vertical DO transport through the bottom is usually a negative value (a sink of DO). The net advective DO flux (Fig. 10a) is much lower in magnitude and biased towards positive values. The time series of net advective DO flux is determined primarily by the currents and not by the DO variations, as is evident by the close resemblance between it and the time series of the horizontal volume transport (dashed line in Fig. 10a). Because of the rotor "pumping" problem with the Aanderaa RCM4 current meters, the volume flux and consequently the advective DO flux is overestimated by as much as a factor of two. However, the zero-crossings and frequency content of the time series should not be affected.

A comparison of the time series of advective flux with that of the daily change in total DO content (Fig. 9b) reveals that some similarities are evident during the period from April to September 1987, although the amplitudes of the advective changes are relatively larger. Positive daily changes in total DO content are coincident with positive advective DO fluxes. Positive (negative) advective fluxes are usually correlated with net volume inflow (outflow) through the cross section at station #20; this means that the vertically averaged DO concentration at station #20 is usually larger than is the horizontally averaged DO concentration at the bottom (25 m) of the control volume. Cross spectral analysis of the 140 day period from April to September 1987 shows that the two time series are coherent (Fig. 11). The coherent bands in the 10 - 20 day and 5 - 6 day period range are also the most energetic bands of the spectra of both time series (Fig. 11). The phase lag

in the coherent bands is small.  During the winter period from November 1986 to April 1987 the calculated correlation is weak and only in the 10 - 20 day period band is there significant coherence.  The weekly (rather than 3-day) sampling period for station #20 DO data during the winter period may obscure the correlation.

Although the advective flux was anticipated to be an important term in the DO budget the detection of the correlation in the data was somewhat surprising for two reasons; 1) The sampling utilized in gathering the DO data was coarse and irregular in space and time, and  2) The speed data obtained by Aanderaa RCM4 current meters was amplified by the mooring motions induced by the surface buoy.  The fact that a significant correlation was found, despite the above mentioned limitations in the data, indicates that the advective flux is  an  important,  if  not  the  dominant  term,  in  the  DO  budget.

Effluent Oxygen Demand

The oxygen demand produced by the mill effluent is caused primarily by the biological stabilization of the more easily metabolized organic constituents by a variety of aerobic microorganisms which utilize them as food.  Metabolization of these organics provide energy and additional biomass for the microorganisms, as well as stable end products such as $CO_2$ and $H_2O$. An immediate chemical oxygen demand (IOD), which may be as large as 11% of the actual BOD, has been reported by Tyler and Gunter (1948) and Poole et al (1978).  However no specific information about the IOD of the Port Alice pulp mill effluent is available.

The process of the stabilization (degradation) of the organic matter in the effluent is often modelled as a first-order reaction.  In such a reaction, the rate is directly proportional to the amount of organic matter C(t) remaining once a suitable population of microorganisms has been reached.  Thus

$$\frac{dC(t)}{dt} = - K \cdot C(t) \qquad\qquad (5)$$

where K is the reaction constant that characterizes how easily the organic matter is metabolized by the microorganisms.  Integrating the above equation in time yields

$$C(t) = C_o \cdot e^{-Kt} \tag{6}$$

where $C_o$ is the initial concentration of organic matter.

Since DO is the parameter of interest the BOD (Biochemical Oxygen Demand) test was developed to quantify the amount of oxygen consumed by the microorganisms during the stabilization of a known quantity of effluent. The BOD test is a bioassay procedure conducted under standardized conditions of temperature (20° C), pH, seed material, dilution and time lag (5 days) and because of this has many well known deficiencies (Sherrard et al 1979). The BOD test measures the amount of DO consumed or exerted rather than the oxygen demand potential remaining. Thus equation (6) for the time decay of the organic matter may be restated in terms of BOD,

$$BOD(t) = L_M \cdot (1 - e^{-Kt}) \tag{7}$$

where $L_M$ is the ultimate BOD potential of the effluent, and is equivalent to $C_o$ since oxygen is consumed in direct proportion to the amount of organic matter oxidized. At the Port Alice mill, the effluents oxygen demand is monitored daily by the BOD(5) test. In order to quantify the DO demand of the accumulated effluent in the fjord, we must determine either the total amount of readily biodegradable organic matter in the receiving waters or the total BOD of the effluent in the fjord. No measurements of this kind are taken in Neroutsos Inlet because of the expense in both time and money that would be involved in such an ambitious monitoring program.

The maximum DO demand of the effluent can be estimated if it is assumed that all of this demand is exerted within the control volume. The validity of this assumption is dependant on the relationship between the exchange time for the control volume and the time characterizing the biochemical reaction that is used to model the decay of the organic matter. Thus if the flushing or exchange time (defined as the control volume divided by the volume flux) is larger than the time constant ($K^{-1}$) of the decay of organic matter, then the above assumption is reasonable because most of the organic matter will be oxidized within the volume before it is flushed out of the fjord. Estimates of the exchange time (uncorrected for speed bias) for the volume, derived from the time series of net horizontal volume flux (Fig. 10a), average about 4 days, but during storms the complete volume can be exchanged in one day. Assuming that the currents may be overestimated by as much as a factor of two, the shortest exchange time is about 2 days and the average time about 8 days.

To quantify the maximum BOD potential of the effluent in the fjord, the daily BOD(5) data (Fig. 12a) was first converted to ultimate BOD loading using equation (7), as follows,

$$L_M = \frac{BOD(5)}{(1 - e^{-K \cdot 5})} \quad . \tag{8}$$

Then the daily input of ultimate BOD to the fjord was accumulated and the total amount allowed to decay as described by equation (6). The oxygen consumed in a given day is then the BOD potential remaining (Fig. 12b) times the rate constant of the first order reaction. Because the rate constant K for untreated sulfite pulp mill effluent is not well known and is apt to change depending on the grade of pulp being produced, a range of values from $K = 0.5$ to $0.2$ d$^{-1}$ was used. A rate constant of $K = 0.22$ d$^{-1}$ is inferred from the work of Tyler and Gunter (1948) and Rennerfelt (1958), but its applicability to the Port Alice mill is unknown. The resulting time series of maximum daily DO demand (Fig. 12c) does not change drastically over the range of K values used in its calculation (average value of $-101 \times 10^3$ kg $O_2$ d$^{-1}$ for $K = 0.5$ d$^{-1}$ versus $-129 \times 10^3$ kg $O_2$ d$^{-1}$ for $K = 0.2$ d$^{-1}$). Low K values result in a higher total BOD potential (because the decay rate is low), and higher K's are associated with lower potential. When daily consumption is calculated, the product of a low K value and a high total BOD potential is not too different from the product of a high K value and a low total BOD potential.

Because equations (1) and (2) are coupled through the terms representing the organic decay and the resulting oxygen consumption, the same advective processes which transport DO into or out of the control volume will also transport organic matter and, in so doing, will influence the character of the time series of effluent DO demand. Thus this time series would (if we could measure it) contain fluctuations related to the advective processes, in addition to those determined by the decay and supply of organic matter.

The time series plotted in Fig. 12c contains only the decay and supply terms. Consequently it has a much lower frequency content than does that of the daily change in total DO content (Fig. 9) - there is no apparent similarity between them. The maximum effluent demand is at times as large as $225 \times 10^3$ kg $O_2$ d$^{-1}$, but typically falls in the range of 100 to $200 \times 10^3$ kg $O_2$ d$^{-1}$. The effluent demand in the latter half of the time series is noticeably larger than that in the first half because BOD(5) output is larger and there were fewer interruptions in production. There are many instances when the daily decline in DO content is greater than the maximum possible effluent demand. In about 50% of these, there is a negative advective flux

which may help to account for the large decline. However, for the remaining 50% there are no readily apparent explanations.

Air-sea Oxygen Flux (Aeration)

The exchange of oxygen across the air-sea interface, termed aeration, is driven by the difference between the oxygen concentration in the overlying atmosphere and that in the seawater. For an unreactive gas like oxygen the resistance to transfer occurs in the liquid phase. The solubility of oxygen in seawater is low. The flux of oxygen across the air-sea interface is given by

$$JO = K_1 \cdot \rho_W \cdot (DO_{sat} - DO) \tag{9}$$

where $K_1$ is the transfer or piston velocity, $\rho_W$ the density of seawater, $DO_{sat}$ is the saturation concentration of oxygen dissolved in seawater, and JO is the diffusive flux of oxygen in the thin liquid film at the surface. The dependance of $K_1$ on wind speed is recognized but the relationship is not well understood. Coantic (1986) has developed an expression for $K_1$, assuming that the air-sea interface is clean and that the winds are not strong enough to result in intense wave breaking. Under these conditions the transfer velocity is given by

$$K_1 = 4.1 \times 10^{-5} \cdot (100 \cdot U_*)^{2.43} \tag{10}$$

for $U_*$, in the range $10^{-3}$ to $6 \times 10^{-2}$ m s$^{-1}$. $U_*$ is the friction velocity in water defined as

$$U_* = (\tau/\rho_W)^{1/2}$$

where $\tau$ is the wind stress. Equation (10) was determined for gases having a Schmidt number of ~600; consequently it was scaled for the Schmidt number of oxygen at 10 °C. The calculation of JO requires the intermediate calculation of $K_1$ as given above, which in turn requires the calculation of $U_*$. The algorithm of Large and Pond (1981) was used to calculate the wind stress using the wind speed, and air and water temperatures measured at mooring SM1 with the Aanderaa weather station. The calculation of the saturation oxygen content in the interfacial layer depends upon the temperature and salinity in this layer. The algorithm of Benson and Krause (1984), together with the temperature and salinity data from 5 m at mooring SM2, was used to calculate $DO_{sat}$. The concentration of dissolved oxygen in the bulk of the fluid was computed by taking the horizontally averaged surface DO data from the mill

water quality surveys. The surface measurements of DO were taken 5 to 10 cm below the surface, well below the thin interfacial layer. The total daily transport of oxygen through the air-sea interface from the head to station #20 is given by the product of JO and A.

The calculated values of $U_*$ are within the range for which Coantic's model is applicable. The difference in concentration of DO between the interfacial layer and that in the bulk of the fluid is due to the fluctuations in the latter (Fig. 13a) as the saturation concentration varies only slightly ($9 \pm 0.5$ ppm) over the 400 day span of the data. As expected, aeration is a source of DO to the fjord - except for two instances (January and May, 1987) when oxygen is being degassed. The total daily transport of oxygen through the air-sea interface of the fjord ( Fig. 13c) has peak values of about $200 \times 10^3$ kg $O_2$ $d^{-1}$ but values are generally less than $100 \times 10^3$ kg $O_2$ $d^{-1}$. A comparison between the daily change in the total DO content (Fig. 9b) and the aeration rate (Fig. 13c) is inappropriate because the wind only mixes the water column over the top 4 to 5 m. A comparison of the daily change in the total DO content of the top 4 m (Fig. 9c) with aeration rate indicates that the latter is much larger and there is no apparent visual correlation between the two signals.

Sediment Oxygen Demand (SOD)

The decomposition of the accumulated wood solids (pulp fibres and bark) and dead microorganisms on the bottom exerts an oxygen demand on the overlying waters. The rate at which the oxygen demand is exerted depends upon a number of factors: temperature, concentration and concentration of wood wastes, pH, etc. In their review of the effect of the pulp and paper industry on the aquatic environment Poole et al (1878) produced a compilation of oxygen uptake rates of marine sediments containing pulp fibres. In situ measurements of oxygen uptake rates ranged from 0.9 to 3.6 g $O_2$ $m^{-2}$ $d^{-1}$.

The total SOD in the control volume is estimated by taking the product of the uptake rate and the overall area of sediments bounding the volume. This bounding sediment area is that of the bottom in the depth range from the surface to 25 m. It is estimated by assuming a 150 m wide band of sediment extends along both shores from the head to station #20, an overall distance of 30 km, which gives a sediment area of $4.5 \times 10^6$ $m^2$. Assuming an average uptake rate of 2 g $O_2$ $m^{-2}$ $d^{-1}$ for all the sediment area estimated above, a SOD of $9 \times 10^3$ kg $O_2$ $d^{-1}$ is calculated.

In terms of the overall DO budget of the inlet, the SOD appears to represent only 7 to 9% of the maximum daily effluent DO demand. However, it

may be a significant sink term, especially in localized areas such as the head where the ratio of sediment area to volume is larger and there are extensive fibre beds.  The occurrence of the lowest DO concentrations at the head may in part be due to the SOD there.  Vertical profiles of DO taken with a polarographic sensor clearly show a rapid drop in DO concentration to near zero values in the bottom few metres at those station taken at the head.

Other Sources and Sinks

Horizontal eddy fluxes in fjords are often assumed to be of secondary importance relative to the advective fluxes (Farmer and Freeland, 1983) and are consequently only discussed briefly here.  The difficulty in assessing the importance of the horizontal eddy flux results from the long-standing problem of determining the representative horizontal eddy diffusivity, $K_H$.  At station #20, (0 to 25 m depth) the total horizontal eddy transport of DO across the vertical cross section $A_{\#20}$ is given by

$$\text{Total eddy flux} \quad = \quad K_H \cdot \frac{dDO}{dx} \cdot A_{\#20} \cdot \rho_w . \qquad (11)$$

Because the DO values at station #20 are almost always larger that those at station #14, the eddy DO flux term is usually source term.  The difference in vertically averaged DO concentration between these two outer stations is at most 3 ppm, but typically about 1 ppm.  Assuming a $K_H$ value of about 100 $m^2$ $s^{-1}$ ($10^6$ $cm^2$ $s^{-1}$) and a change in DO of 1 ppm over the 6 km distance between stations #14 and #20 the horizontal eddy flux of DO is about 50 $\times$ $10^3$ kg $O_2$ $d^{-1}$.

The vertical eddy flux estimates are plagued by the same problem - the determination of the eddy diffusivity.  The total vertical eddy flux of DO through the bottom surface (at 25 m), A, of the control volume is given by an expression analogous to that in equation (11),

$$\text{Total Vertical Eddy DO Flux} \quad = \quad K_V \cdot \frac{dDO}{dz} \cdot A \cdot \rho_w . \qquad (12)$$

The vertical eddy flux, unlike the horizontal flux, can be either a source or sink of DO since the vertical gradient between 20 and 25 m changes sign frequently.  The size of the gradient in absolute terms is usually less than 1 ppm in 5 m.  Choosing a $K_V$ value of 1 $\times$ $10^{-4}$ $m^2$ $s^{-1}$ (1 $cm^2$ $s^{-1}$), and a vertical gradient of $\pm 1$ ppm $O_2$ in 5 m gives a total vertical eddy DO flux of $\pm 30 \times 10^3$ kg $O_2$ $d^{-1}$.

Both the horizontal and vertical fluxes appear to be appreciable terms in the DO budget, but until accurate estimates of the eddy diffusivities are made the actual importance of these terms remains in question.

## V BOX MODEL

In this section a simple box model is constructed for the DO and effluent content of the fjord. The dominant sources and sinks examined in section IV are included in simplified form, and parameters describing these terms are varied so as to determine their effects on the results. The purpose of this modelling exercise is to gain a better understanding of the effects that alteration of the rate constant for the BOD and of the flushing times of the control volume will have on the solution. As was pointed out in section IV, the rate constant of the BOD reaction is not well known, and there are no reliable current meter data from which to infer accurate flushing times. By making informed guesses about the amount of BOD loading, the rate constant, the flushing times etc., the model results can be compared to the observed DO depressions. This should indicate whether such a simple model can reproduce the observations.

The ultimate BOD accumulated in the control volume is described by the following equation which is essentially a restatement of equation (1) with replacement of the biodegradable organic matter by the equivalent ultimate BOD:

$$\frac{dL}{dt} = U \cdot (l_o - l) - K \cdot L + L_M \tag{13}$$

where L is the accumulated ultimate BOD, $l_o$ is the ultimate BOD concentration in the outside waters, $l$ is the average ultimate BOD concentration in the fjord, $L_M$ is the daily input of ultimate BOD to the fjord by the pulp mill, K is the BOD reaction constant, and U is the volume exchanged daily between the control volume, V and the outside waters. The diffusive flux of ultimate BOD between the control volume and the outside waters is not included. The solution of equation (13), assuming that the daily volume exchange and mill BOD input are constant, is

$$L(t) = (L_o/T + L_M) \cdot (1 - e^{-\alpha t})/\alpha + L_o \cdot e^{-\alpha t} \tag{14}$$

where $\alpha$, the effective rate constant, is the sum of the exchange rate, $1/T = U/V$ (inverse of flushing time), and the rate constant of the BOD reaction, i.e. $\alpha = (1/T + K)$. $L_o$ is the initial accumulated BOD, and we can

assume that ultimate BOD of the waters outside of the volume is small. Thus if $L_O = 0$ then the solution becomes

$$L(t) = (L_M/\alpha) \cdot (1 - e^{-\alpha t}) \qquad (15)$$

For $t \gg 1/\alpha$ then $L(t) \approx L_M/\alpha$, which is just the daily input of ultimate BOD times the effective time constant for the combined decrease in BOD caused by the advective exchange and biochemical decay. In the case of very long flushing times, i.e. of very small or no exchange, the steady state accumulated BOD in the box becomes simply $L_M/K$ and the daily oxygen demand exerted by the effluent is exactly balanced by the daily ultimate BOD input from the pulp mill.

The oxygen balance given by

$$\frac{dO}{dt} = U \cdot (DO_O - DO) - K \cdot L - SOD \qquad (16)$$

is a simplified version of equation (2), where $DO_O$ is the dissolved oxygen concentration of the outside waters and DO is the average dissolved oxygen concentration in the fjord. The first term on the right hand side represents the advective DO flux, the second the oxygen demand rate of the accumulated effluent, and the third the sediment oxygen demand rate. The diffusive flux of oxygen and aeration have been neglected. The solution of equation (16) assuming a constant SOD is

$$O_O - O(t) = T \cdot SOD \cdot (1 - e^{-t/T}) + L_M \cdot (K \cdot T + e^{-\alpha t})/\alpha - T \cdot L_M \cdot e^{-t/T} \qquad (17)$$

where $O_O$ is the initial total oxygen content. The solution above is written such that the left hand side represents the total DO depression or deficit relative to the background or initial conditions. The first term on the right hand side is the contribution to the DO deficit from the sediment oxygen demand and the last two terms are the contribution from the effluent's oxygen demand. The above equation describes the development in time of the DO deficit, from an initially unpolluted state. Of interest is the steady state DO deficit which for $t \gg 1/\alpha$ approaches the following solution

$$O_O - O = T \cdot SOD + L_M \cdot K \cdot T^2/(K \cdot T+1) . \qquad (18)$$

Equation (18) can be written in terms of the daily BOD(5) discharge using equation (8)

$$O_o - O = T \cdot SOD + BOD(5) \cdot K \cdot T^2/[(1 - e^{-K \cdot 5})(K \cdot T + 1)] \qquad (19)$$

so that the dependance of the steady state solution upon the rate constant, flushing time, BOD(5) loading, and SOD rate is explicitly shown. In Fig. 14, the variation in the factor that multiplies BOD(5) in equation (19) is plotted against flushing time T for a variety of decay constants. For flushing times of up to 5 days the decay constant of the BOD reaction is not important. However, as the flushing time increases beyond 5 days, the factor becomes increasingly sensitive to changes in the decay rate. Also, the contribution to the oxygen deficit from the SOD increases in direct proportion to the flushing time T.

Attempts to verify the relationship between oxygen deficit and BOD(5) have been frustrated because the necessary information about the flushing time of the inlet, the BOD reaction rate and SOD rate is either lacking or poorly described. The flushing time T is a key parameter, as is evident from Fig. 14, and also fluctuates greatly on a variety of time scales. One may attempt to use the model with data averaged over sufficiently long time spans (e.g. annual), in which case it may be argued that the average flushing time, BOD reaction rate and SOD should not change significantly from one year to the next.

In the present case, a flushing time of about 11.5 days ($K = 0.25$ d$^{-1}$) is required to reconcile the average oxygen deficit ($1 \times 10^6$ kg O$_2$) for the 12 month period starting November, 1986 with the average BOD(5) daily input of $76 \times 10^3$ kg O$_2$ for the same period. This flushing time compares favourably with the estimate of the volume flushing time of 10 days, for the same period, obtained from the current meter data. The contribution of the SOD to the oxygen deficit is about 10% for SOD = $9 \times 10^3$ kg O$_2$ d$^{-1}$.

## VI SUMMARY AND CONCLUSIONS

The presentation and examination of the IOS and pulp mill's data sets for Neroutsos Inlet have clearly shown that the most severely affected receiving waters are from station #8 to the head of the fjord, from just below the surface to 25 m depth. In this volume DO levels are on average well below protection level C values - those for which Davis (1975) states "... deleterious effects may be severe ..." on the fish community. The impact of the effluent on the fjord DO levels has been observed beyond station #20, but the magnitude of the DO depressions is considerably reduced there. At station #20 itself the overall DO level is about 0.2 ppm lower than the

overall background level of 7.2 ppm as measured at station Q4 in Quatsino Sound.

In spite of the deficiencies of the current meter data, a general near surface circulation pattern is observed.  It consists of a surface outflow layer and a return flow below this layer - the flow having a zero-crossing between 5 and 10 m.  The EOF analysis of the combined current meter and anemometer data indicates that this general circulation pattern is wind driven.  The general surface outflow is also consistent with an estuarine flow, but no runoff data exist with which to test this hypothesis.  It should be noted that during periods in which storms release large amounts of precipitation on this region strong southeasterly (down inlet) winds are also generally present.

An examination of the daily changes in the DO content of the fjord shows that they range widely, but typical daily increases and decreases are about $150 \times 10^3$ and $-200 \times 10^3$ kg $O_2$ $d^{-1}$, respectively.  The frequency content of the time series of daily change in DO content has broad peaks centred at 15 and 5 day periods.  The advective flux of DO is an important, if not the dominant, source term in the DO budget of Neroutsos Inlet.  However, a quantitative evaluation of the advective flux is precluded by the bias (resulting from the surface buoy motion) in the Aanderaa RCM4 current meter speed data.  The oxygen demand of the pulp mill effluent in the fjord is the dominant sink for DO but it could not be directly estimated.  Instead, the maximum DO demand of the effluent was estimated using a range of first-order rate constants, $K = 0.2$ to $0.5$ $d^{-1}$, by assuming that all of the effluent's potential DO demand was exerted within the control volume.  The magnitude of the sediment oxygen demand term is not well known.  Using an average uptake rate of 2 g $O_2$ $m^{-2}$ $d^{-1}$ for all the sediment area considered, the SOD is about 7 to 9% of the maximum effluent DO demand.  SOD may be important near the head of the fjord, where there are extensive fibre beds, the ratio of bottom surface area to volume is large, and flushing may be more sluggish.

Although the model of Coantic (1986) appears to indicate that the aeration rate is a substantial source term, its importance should be minimized because of the large uncertainty involved in the estimation.  The uncertainty stems from the experimental data used by Coantic (1986) to give the power-law fit of equation (10); the transfer velocity may vary by as much as a factor of four for a given $U_*$.  Estimates of the transfer velocity, $K_1$ may easily change by a factor of two depending on the type of model that is used to fit the experimental data. In the words of Coantic " ... interfacial gas transfer is still far from being well-understood and parameterized ...".  The observations that the aeration term was larger than, and not correlated with, the daily DO

changes in the top 4 m of the control volume suggest that aeration is not a significant source term.

The horizontal and vertical eddy fluxes of DO appear to be relatively minor terms in the overall budget of DO, but since it is difficult to arrive at estimates for the coefficients of both eddy diffusivities their contribution cannot properly be assessed. In the case of the horizontal eddy flux, the gradient in DO is such that this term is almost always a source term, but in the case of the vertical eddy flux the DO gradient can be of either sign, making this term both a source or a sink. The role of oxygen production by photosynthesis is not clear, though it appears it could at times have an appreciable effect.

A box model, which incorporated the main sources and sinks of DO and organic matter, was developed. The model was used to explore the effects of the BOD reaction rate constants, flushing times, BOD loading and SOD on the overall DO content of the fjord. It shows that the effect of changes in BOD rate constants become important for flushing times greater than about 5 days. Although the model could not be verified, the flushing times needed to reconcile the daily BOD(5) loading with the observed deficit are comparable to those estimated from the current meter data.

One of the important objectives of this study is to provide a basis for the determination of the amount of secondary treatment required to reduce both the frequency of occurrence and the severity of low DO events to "acceptable" levels. Assuming that the Davis protection level B (a DO of 6.5 ppm) is an acceptable target value for the secondary treatment measures, how much should daily BOD(5) loading be reduced to achieve this target? This question implicitly assumes that there is a rational basis upon which to provide an answer, i.e. that there is a verifiable relationship or calibrated model which describes the oxygen deficit in terms of the effluent's BOD loading, the flushing time and SOD. The box model presented in Section V provides such a relationship, but, as already mentioned it has not been verified. Furthermore, the model has no spatial or temporal resolution, it treats the problem in an integrated, steady state sense.

Nevertheless, using the box model and assuming that;
a) SOD = $9 \times 10^3$ kg $O_2$ $d^{-1}$,
b) K = 0.25 $d^{-1}$
c) T = 10 days
d) the average background DO level is 7.2 ppm (station Q4),
e) the average daily BOD(5) output of $76 \times 10^3$ kg $O_2$ produces a control
   volume average DO level of 5 ppm (2.2 ppm below background),

then the daily BOD(5) output would have to be reduced to an absolute value of $23 \times 10^3$ kg $O_2$ (_70% reduction) to improve the overall oxygen deficit to only 0.7 ppm below background, and thus achieve (in an average sense) protection level B oxygen values of 6.5 ppm.

The severity of the DO depression and its spatial extent cannot be determined from the box model. However, it is unlikely that the 6.5 ppm level will be achieved near the head of the fjord during the late summer and fall, at which time even background levels (Table 2) fall below this level.

In summary, although the question about the extent of secondary treatment is easy to pose any answer obtainable at present cannot be definitive because it is dependant upon many unknown factors. What is clear is that a substantial reduction in daily BOD(5) output is required before protection level B dissolved oxygen concentration can even be approached. Reduction of the daily BOD(5) discharges to about $20 \times 10^3$ kg $O_2$ would produce substantial improvement but it is unlikely that a DO level of 5 ppm will be achieved at all times.

## VII RECOMMENDATIONS

To move towards a more precise answer will require considerably more research into the areas of effluent characterization, SOD and more detailed monitoring programs, and yet another oceanographic study. Our ability to predict the effects of treatment will never be any better than our ability to verify and model the complex biochemical and physical processes at work in this pollution problem. Because of their practical importance most of these are currently the subject of intensive research in various parts of the world. Recommendations for some specific area of research are:

### Effluent Characterization

Both the analysis of the sources and sinks of DO in the fjord and the ability to model the BOD reaction in the receiving waters has been hampered by the almost total lack of information about the Port Alice pulp mill's effluent oxygen demand. In order to determine how to model the effluent's DO demand in the receiving water, oxygen uptake measurements of the effluent should be obtained under conditions resembling those encountered in the receiving waters (i.e. temperatures more closely resembling those of the fjord (10 °C), seed organisms from the fjord, and effluent dilutions comparable to those encountered in the fjord). Another aspect of the effluent's oxygen demand is the issue of the immediate chemical oxygen demand (IOD) reported by Tyler and

Gunter (1948). Tests need to be done on the effluent to determine if an IOD exist and, if so, to quantify the amount.

Effluent Monitoring

All effluent discharges to the fjord should be monitored and characterized where possible since they are the primary forcing for the low DO observed. The effluent discharge through the diffuser is presently monitored for BOD(5), SSL, and total flow, but sewering from the SSL pond is not. Any other effluent stream discharge to the fjord, accidental or not, should be reported and quantified. Our ability to model the observed DO levels in the fjord will depend upon accurate determinations of the amount and character of the effluent discharged.

Monitoring Program

The monitoring data collected by the environmental staff at the pulp mill have been essential to the analysis of the pollution problem in this fjord. A minor alteration to the stations monitored should result in a better measure of the overall impact of the effluent. This alteration, which involves no additional effort, consists of the elimination of station #5 and the provision of station #17 in its place. Sampling frequency should be maintained at three survey per week from the head of the inlet to station #20, and beyond if low DO conditions are observed at station #20.

Winds have been shown to play a significant role in the near surface circulation, yet reliable wind data are not available on a routine basis. It is recommended that winds be routinely measured and recorded from an exposed location in the inlet, such as Mist Rk. near station #17. The role of runoff in the near surface circulation is anticipated to be significant but no data are available to confirm this hypothesis. It is suggested that runoff to the fjord from the main streams be gauged for a sufficiently long period of time to enable a the runoff regime to be modelled in terms of the local precipitation.

Sediment Oxygen Demand

The sediment oxygen demand term in Neroutsos Inlet is not well known. Its calculation was based on a guess of the appropriate value from a range of oxygen uptake rates reported in the literature. Because the SOD tern could have an appreciable effect on the overall DO content of the fjord, it is important to accurately evaluate this term and examine the contributing factors. The accurate determination of the SOD is a two step process. First, the sediments should be classified by type (based on visual appearance,

organic content, composition etc.) and the area in each classification delineated. Second, in situ oxygen uptake rate measurements representative of each sediment class should be obtained. The SOD term is then be determined by the sum of the contributions from each of the sediment classes.

## VIII ACKNOWLEDGEMENTS

## IX REFERENCES

Barnes, C.A., E.E. Collias, V.F. Felicetta, O. Goldschmid, B.F. Hrutfiord, A. Livingston, J.L. McCarthy, G.L. Toombs, M. Waldichuk, and R. Wertly, 1963. A standardized Pearl-Benson, or nitroso, method recommended for estimation of spent sulfite liquor or sulfite waste liquor concentration in waters. TAPPI 46(6): 347-351.

Benson, B.B. and D. K. Krause, Jr., 1984. The concentration and isotopic fractionation of oxygen dissolved in freshwater and seawater in equilibrium with the atmosphere. Limnol. Oceanogr., 29(3): 620-632.

Coantic, M. A., 1986. A model of gas transfer across air-water interfaces with capillary waves. J. Geophys. Res., 91(C3): 3925.

Cross, S. F. and D. V. Ellis, 1981. Environmental recovery in a marine ecosystem impacted by a sulfite process pulp mill. WPCF 53(8): 1339-1346.

Davis, J. C., 1975. Minimal dissolved oxygen requirements of aquatic life with emphasis on Canadian species: a review. J. Fish. Res. Bd. Can., 32(12): 2295-2332.

Farmer, D. M. and H. J. Freeland, 1983. The physical oceanography of fjords. Prog. Oceanogr., 12(2): 147-219.

Kutzbach, J. E., 1967. Empirical eigenvector of sea level pressure, surface temperature and precipitation over North America. J. Appl. Meteor., 6: 791-802.

Large, W. G. and S. Pond, 1981. Open ocean monentum flux in moderate to strong winds. J. Phys. Oceanogr., 11: 324-336.

Poole, N. J., D. J. Wildish and D. D. Kristmanson, 1978. The effects of the pulp and paper industry on the aquatic environment. CRC Cri. Rev. Env. Control. pp 153-195.

Poulin, V. A. and E. Oguss, 1982. Migration characteristics of juvenile chum salmon in Neroutsos Inlet with particular emphasis on the effects of sulphite mill effluent on migratory behaviour, 1980. Environmental Improvement at Neroutsos Inlet, B. C., Vol. 4, 45 pps.

Tokar, E. M., J. P. Campbell and R. Tollefson, 1982. Environmental improvement at Port Alice, B. C., Pulp and Paper Can., 83(5): 50-53.

Seaconsult Marine Research Ltd., 1987. Port Alice oceanographic study: Review of data. 42 pps.

Sherrard, J. H., A. A. Friedman and M. C. Rand, 1979. BOD5: are there alternatives available? WPCF, 51(7): 1799-1804.
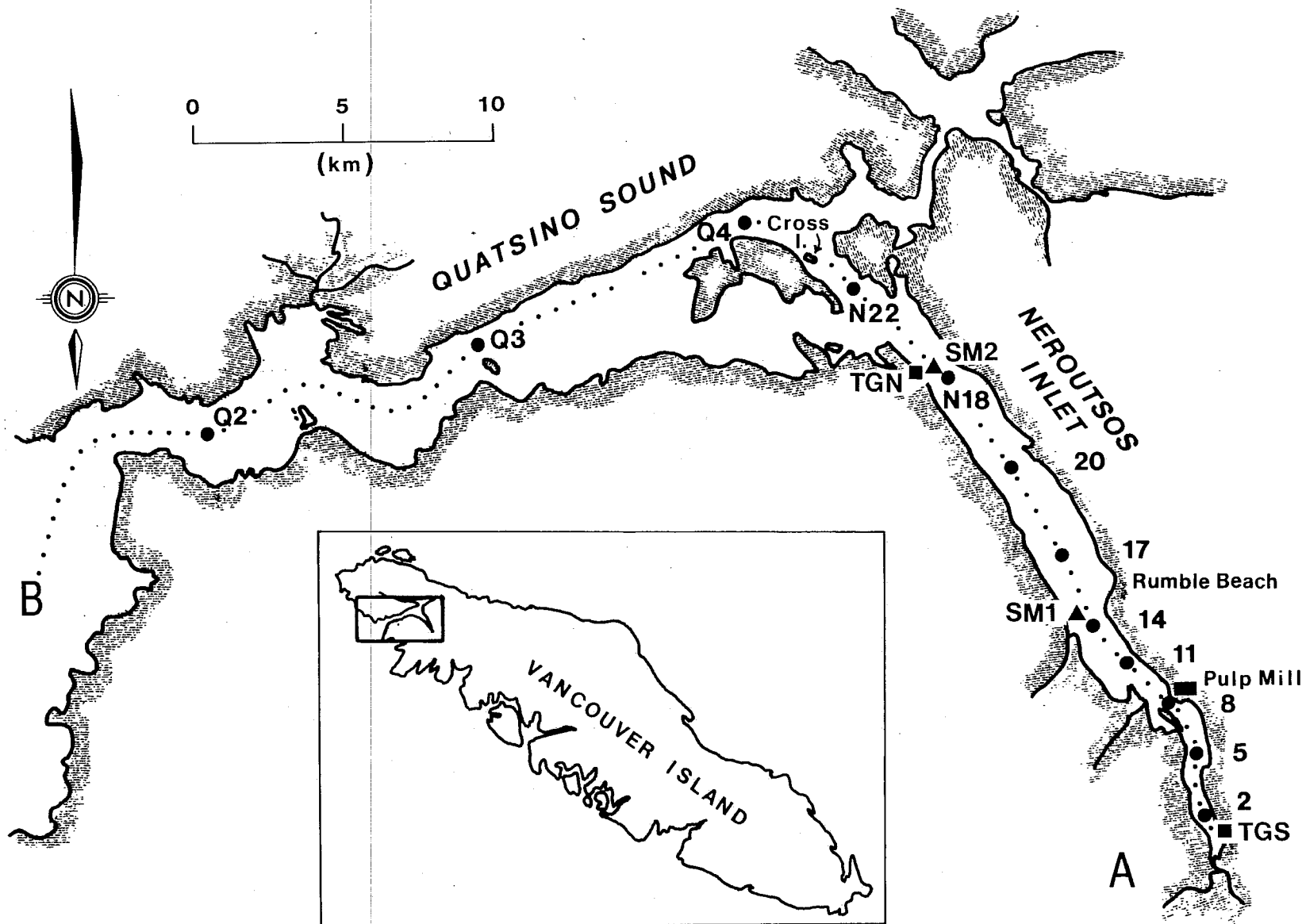
Figure 1. Site map of Quatsino Sound and Neroutsos Inlet showing the locations of sampling stations (circles), surface moorings (triangles) and bottom mounted pressure gauges (rectangles).
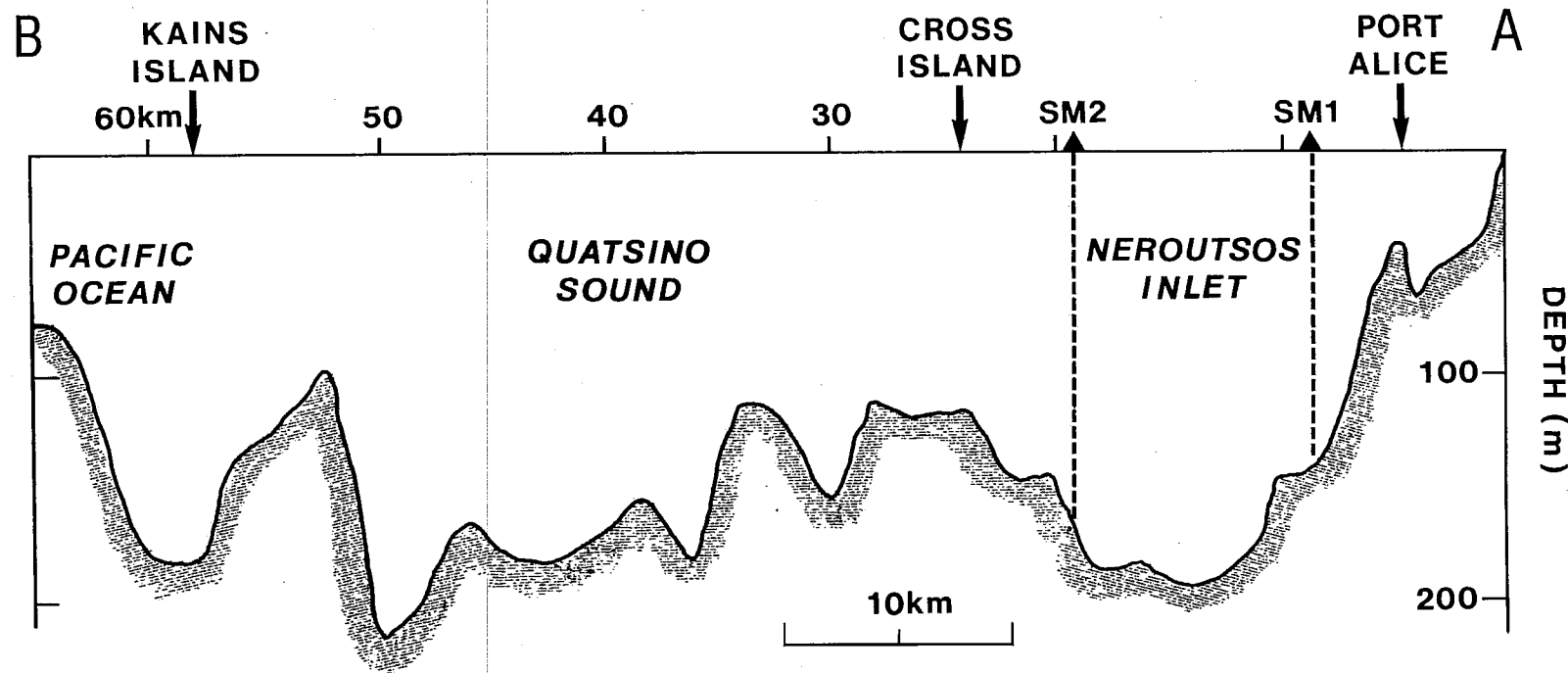
Figure 2. Longitudinal depth profile from the head of Neroutsos Inlet (A) to the mouth of Quatsino Sound (B) showing the location of the surface moorings.
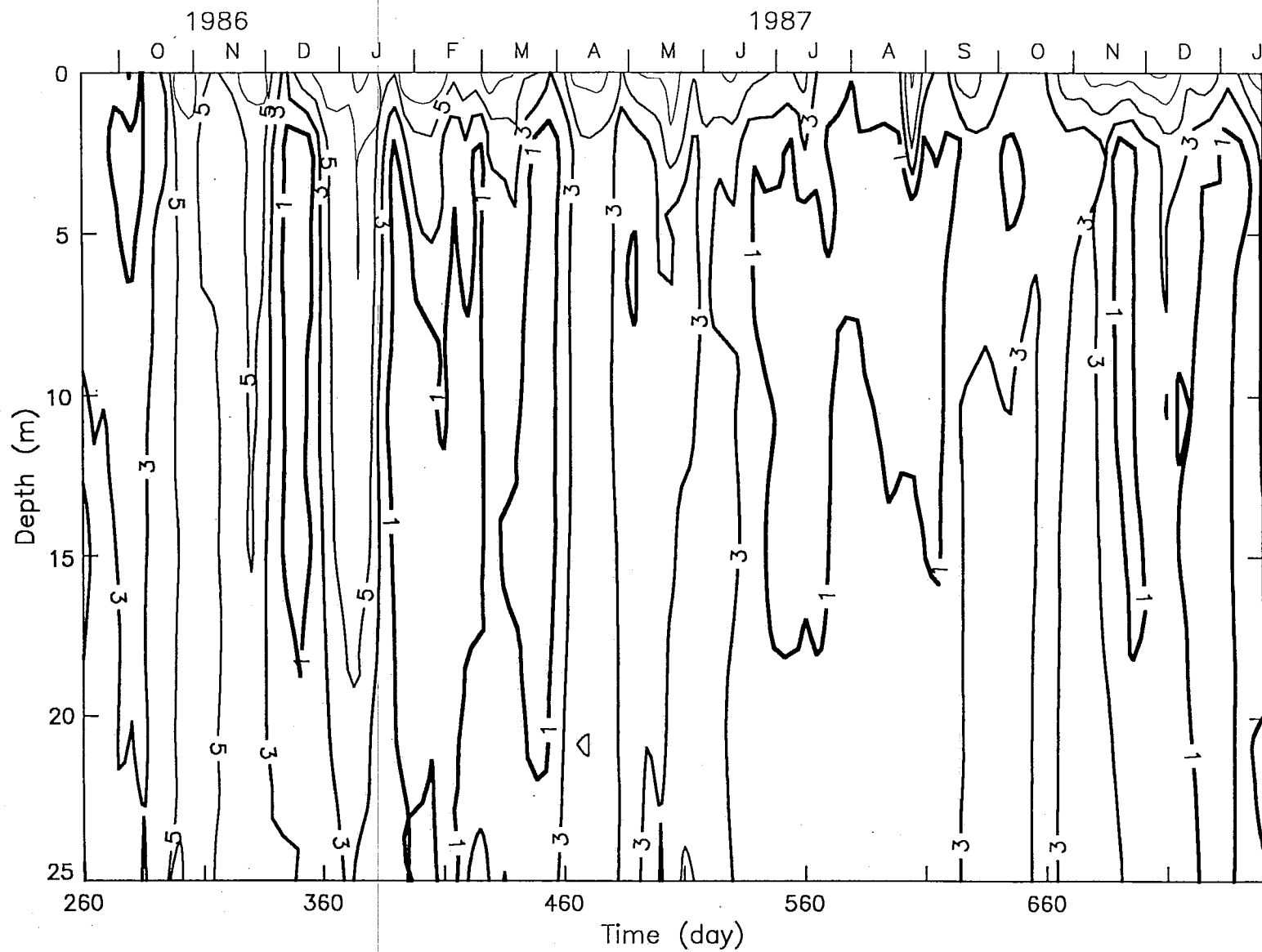
Figure 3. Depth-time contours of DO (ppm) at station #2 from September 1986 to January 1988.
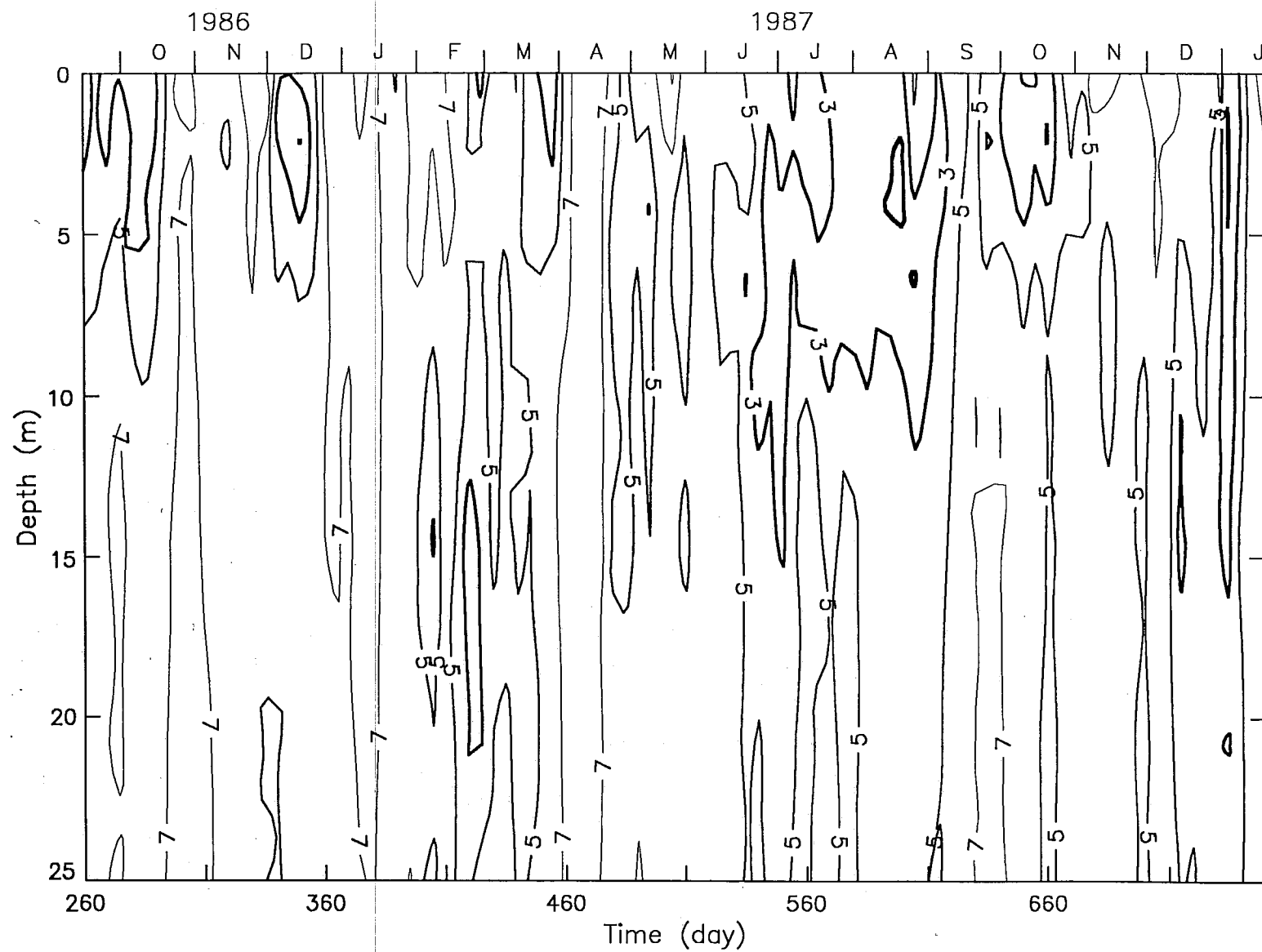
Figure 4. Depth-time contours of DO (ppm) at station #14 from September 1986 to January 1988.
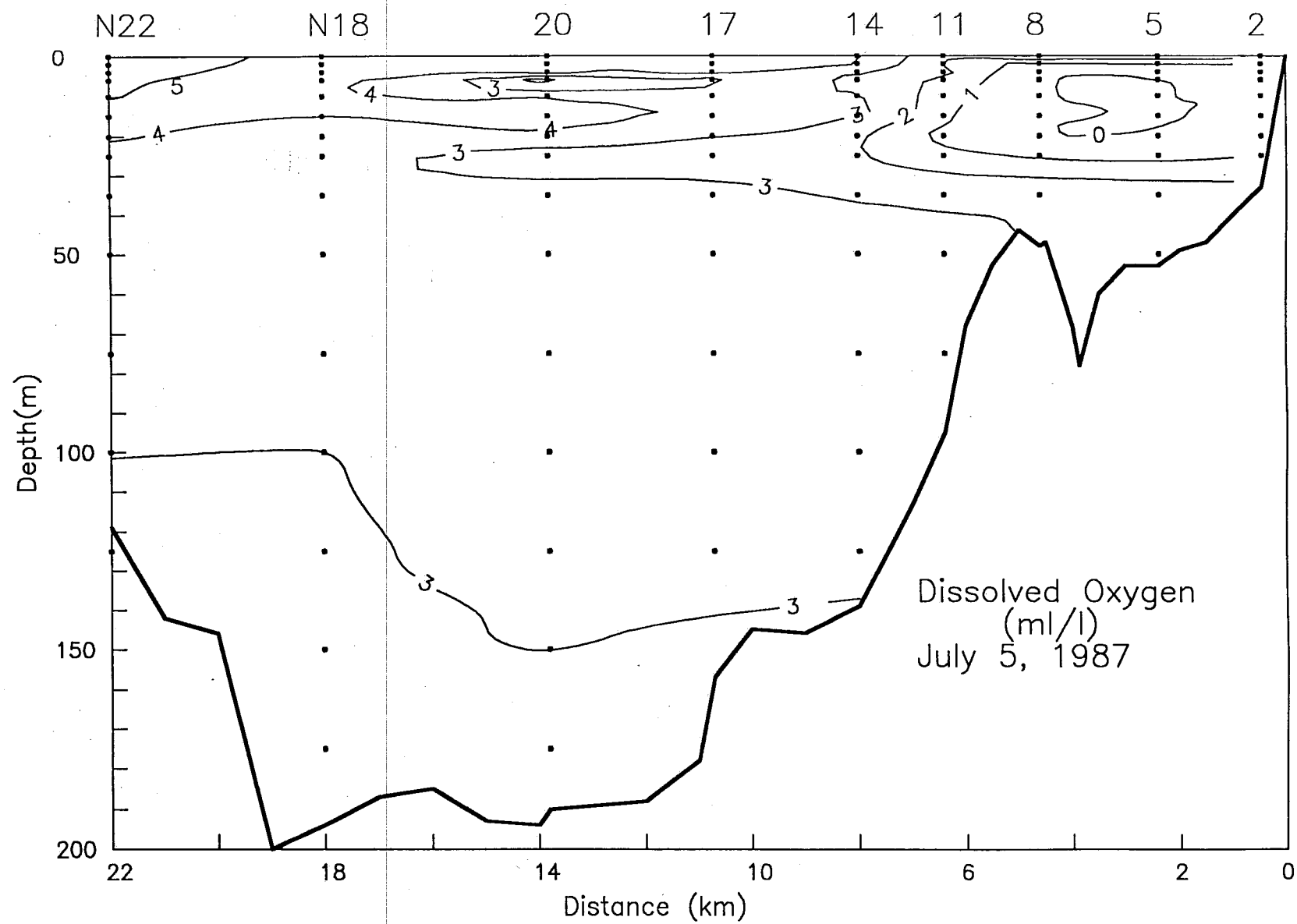
Figure 5. Axial cross sections of DO (ml/l) in Neroutsos Inlet taken on July 5, 1987.
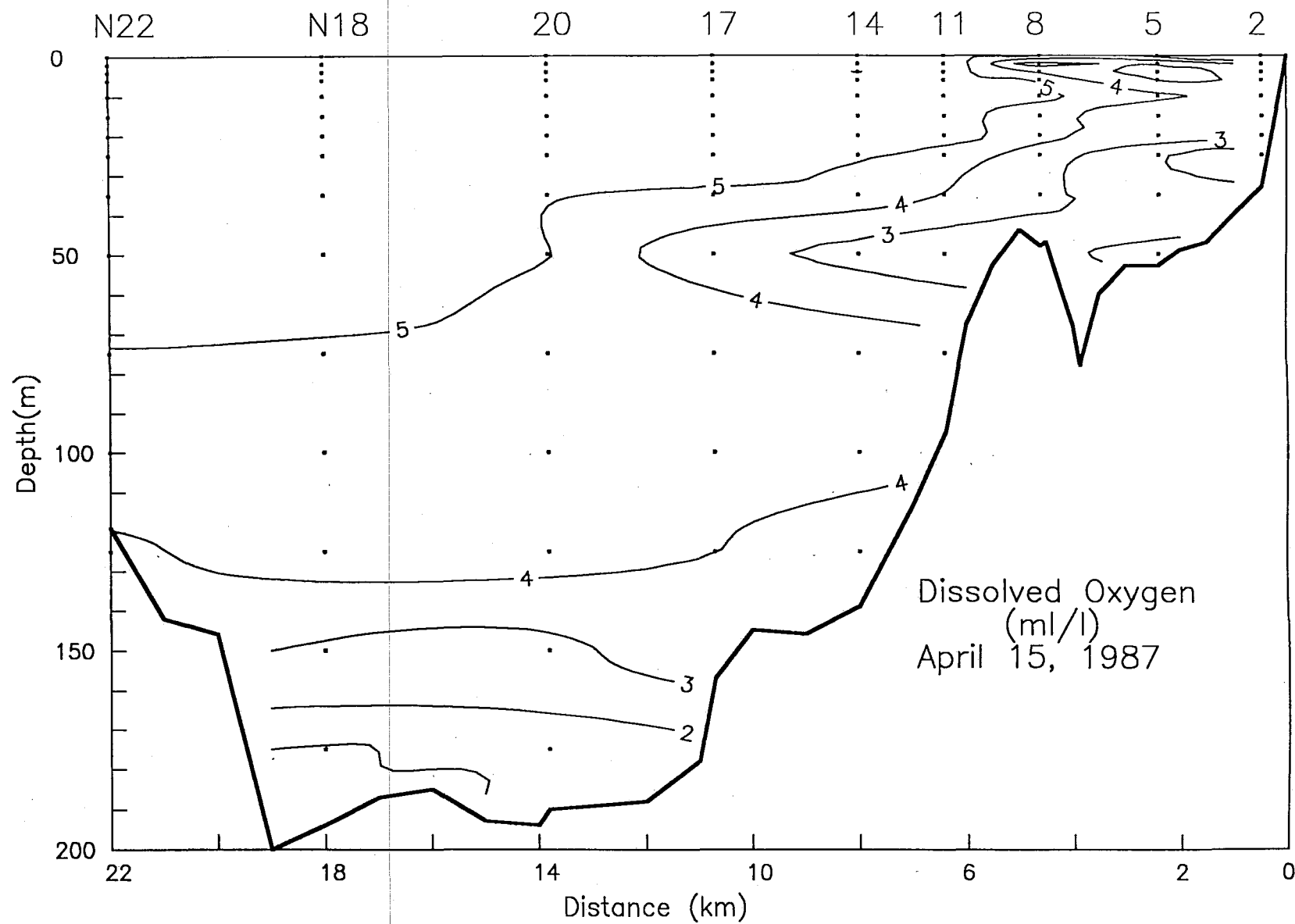
Figure  6.  Axial cross sections of DO (ml/l) in Neroutsos Inlet taken on April 15, 1987.
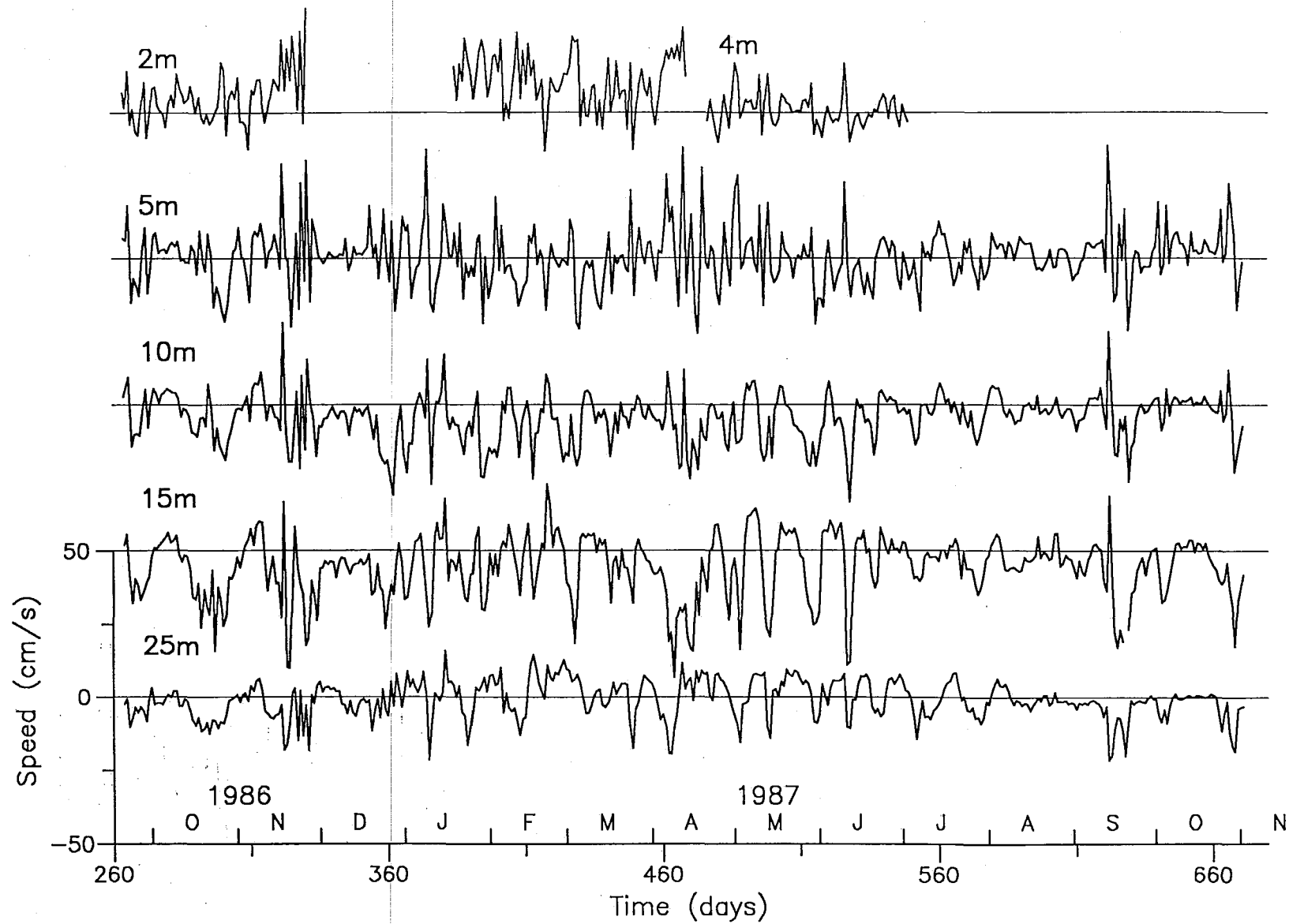
Figure 7. Low-passed currents from mooring SM2, at depths of 2, 5, 10, 15, and 25 m depths, resolved along the channel axis for the period September 1986 to November 1987.
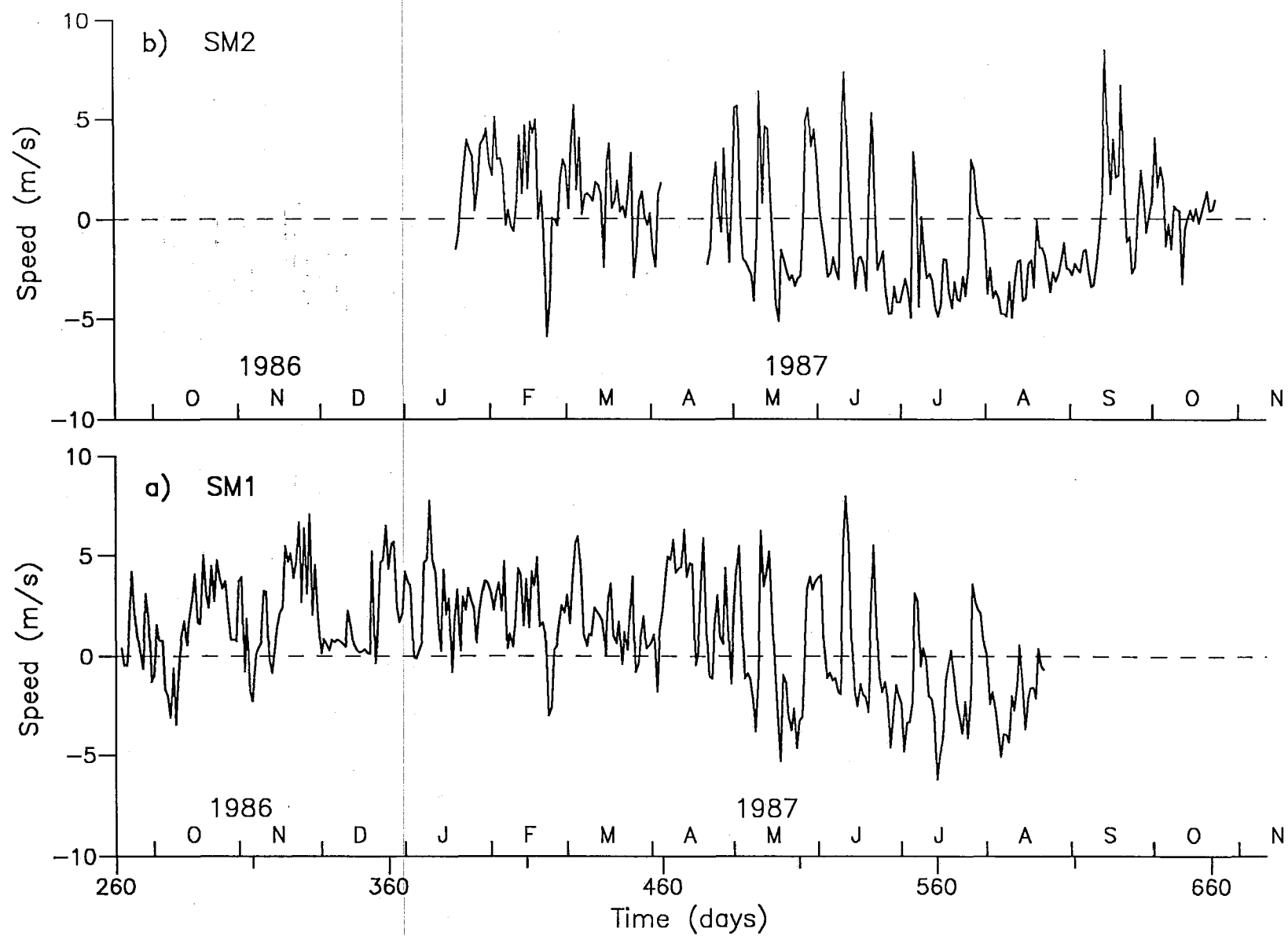
Figure 8. Low-passed wind data from moorings SM1 and SM2, resolved along the channel axis for the period September 1986 to October 1987.

42
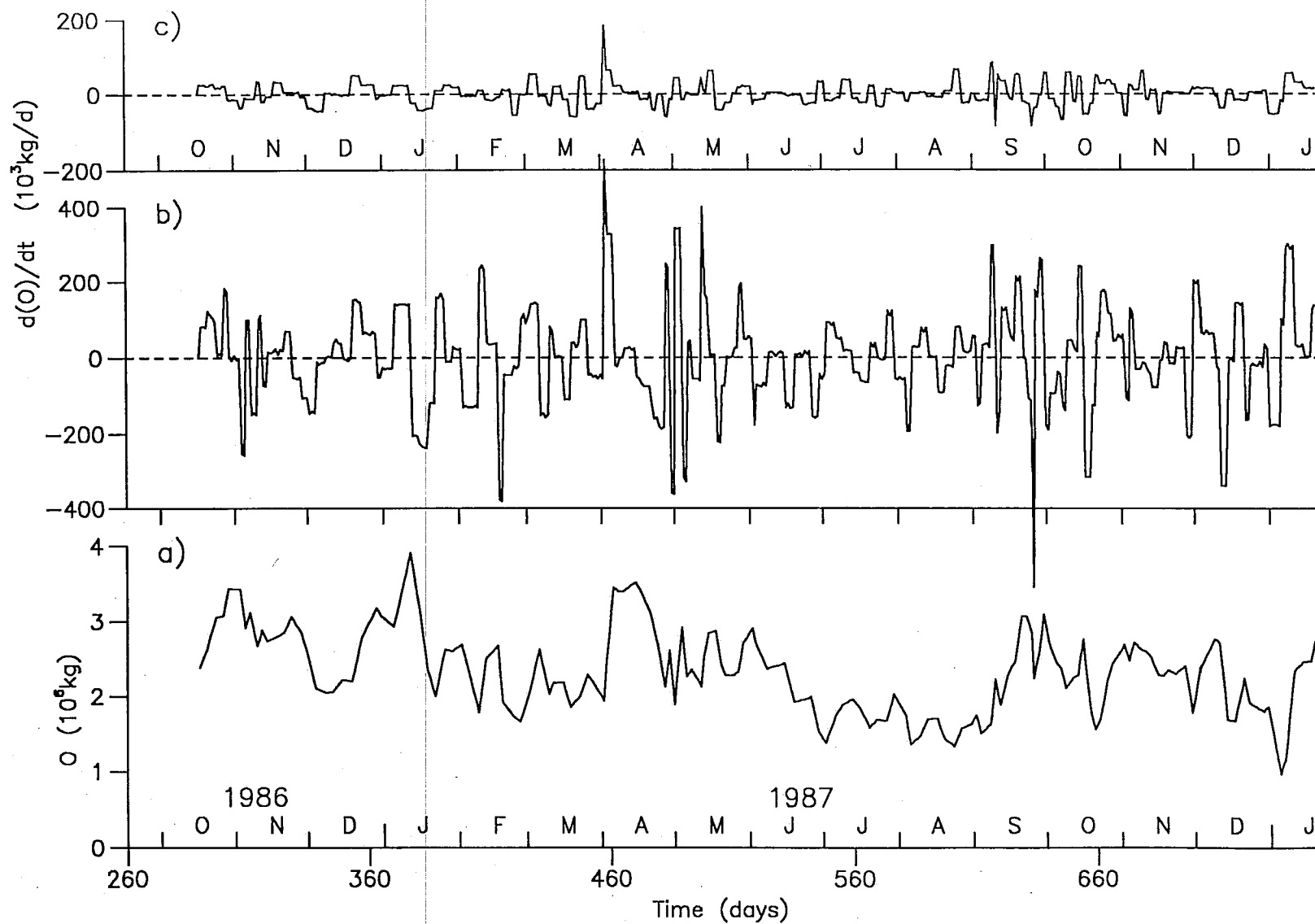
Figure 9. Time series plot of a) total DO content in the control volume, b) daily change in total DO content in the volume, and c) daily change in the DO content from 0 to 4 m.
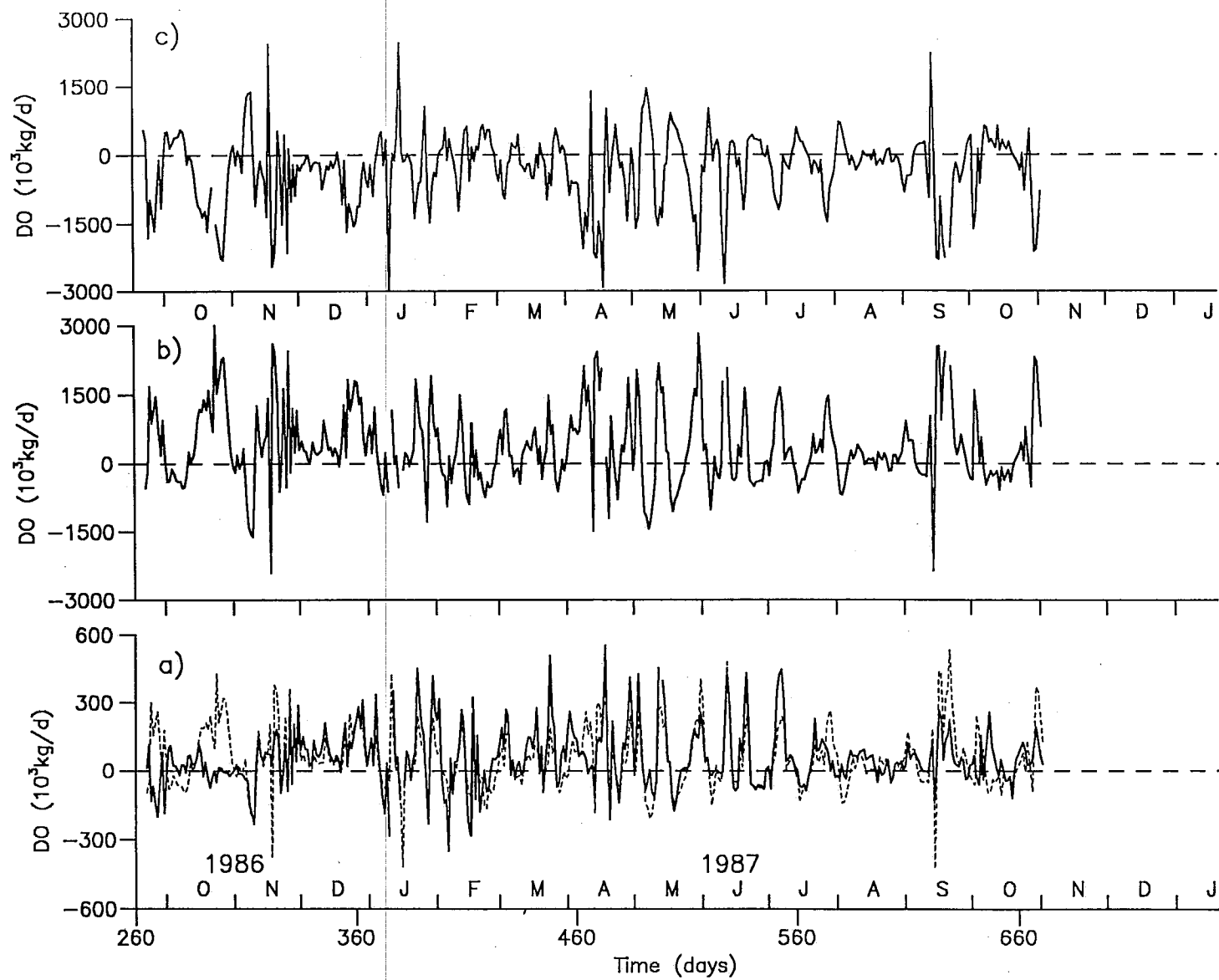
Figure 10.  Time series plot of a) net advective DO flux and horizontal volume transport (dashed line), b) horizontal DO flux, and c) vertical DO flux.
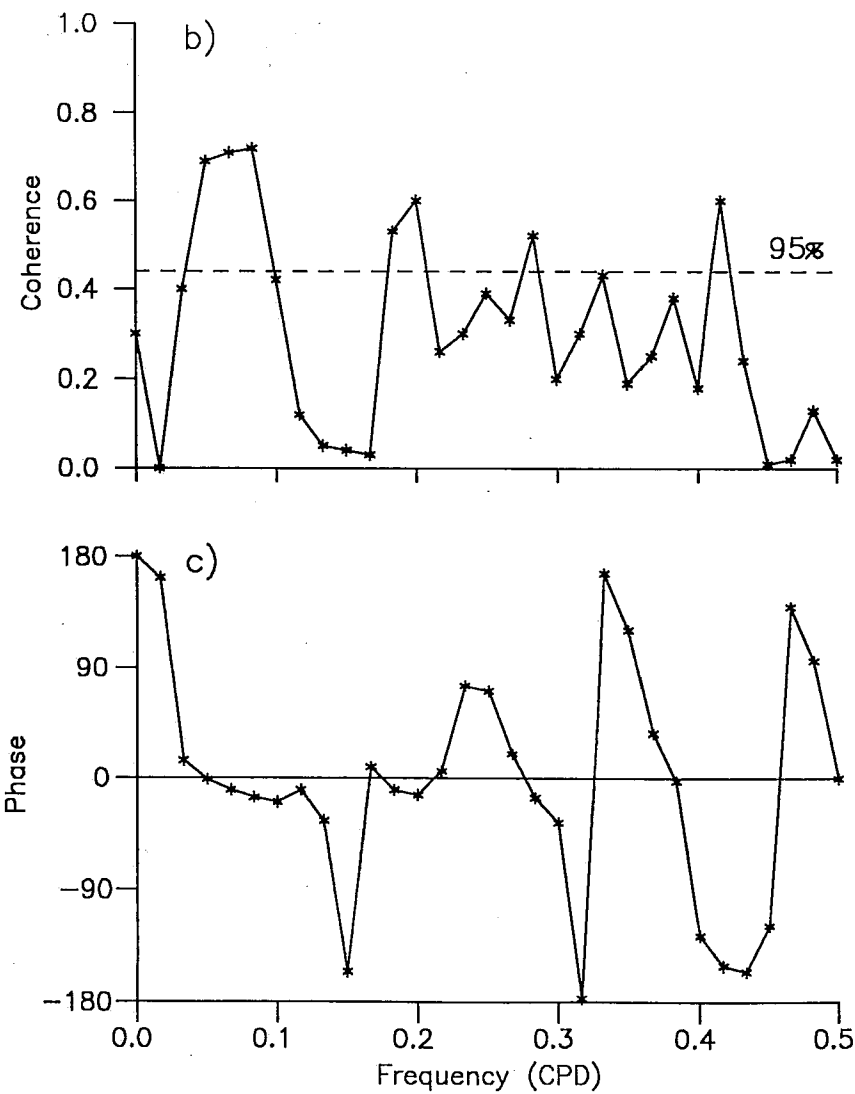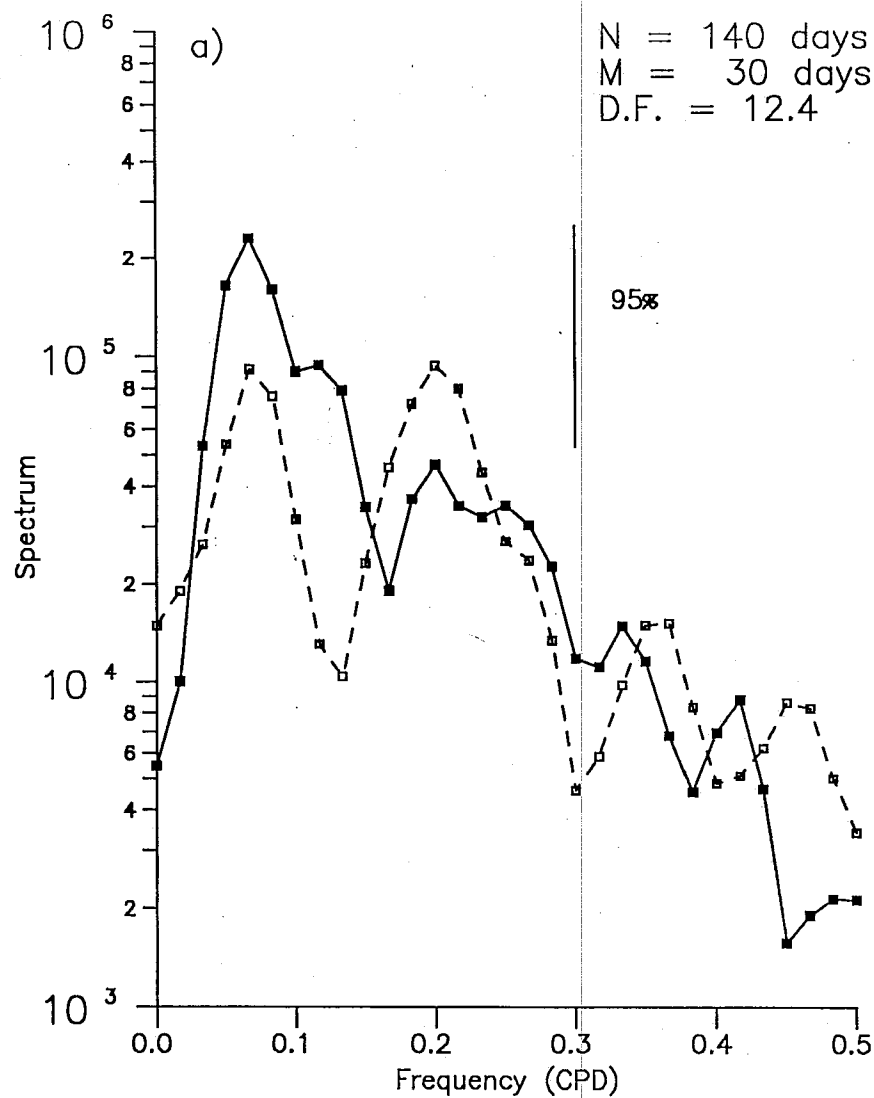
Figure 11. Plots of a) the spectra of the advective DO flux (solid squares) and daily change in DO content(open squares), b) the phase and c) coherence squared spectrum.
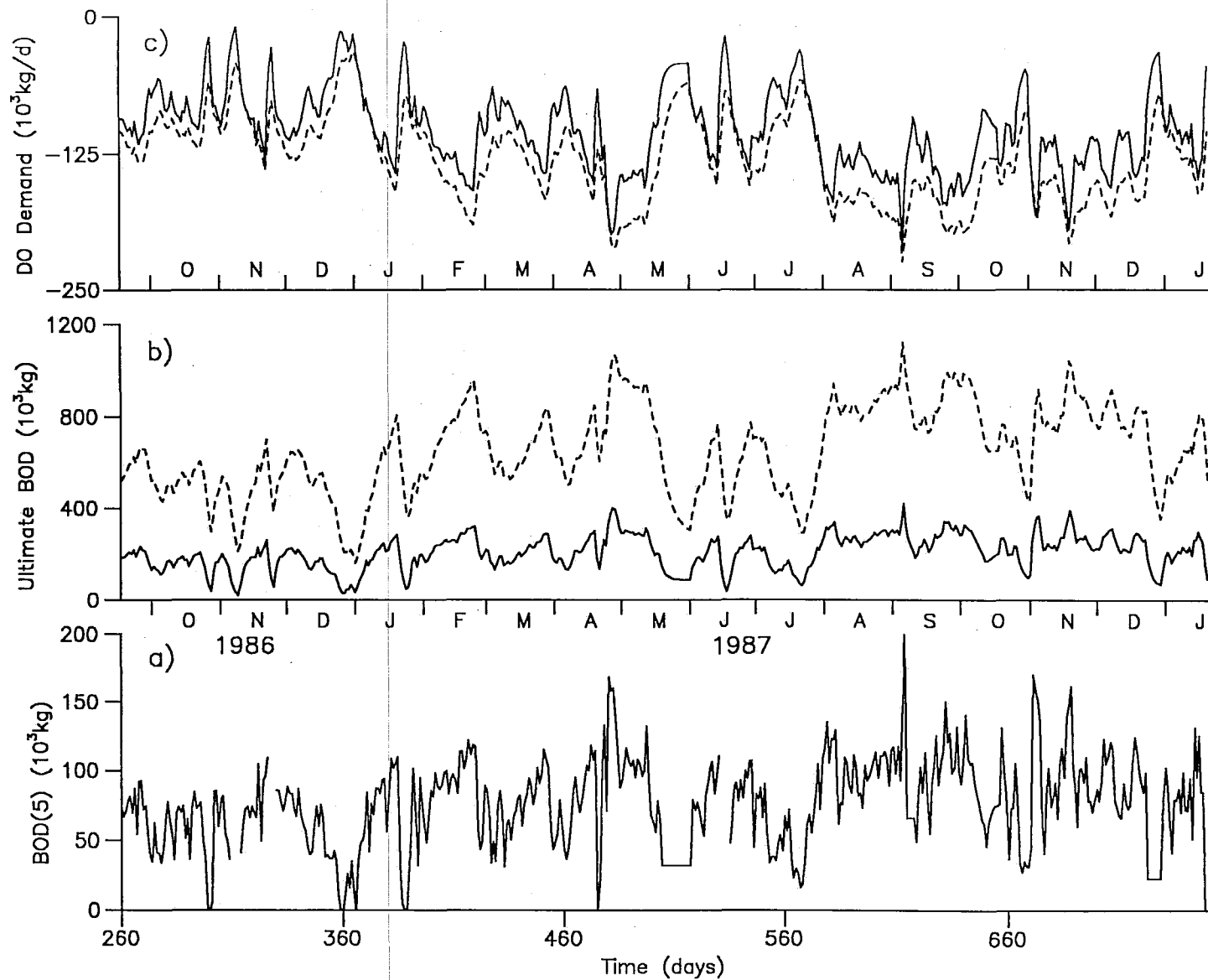
Figure 12. Time series plots of a) daily BOD(5) discharge, b) accumulated ultimate BOD, and c) demand of accumulated effluent for K = 0.2 (dashed) and 0.5 d$^{-1}$ (solid).
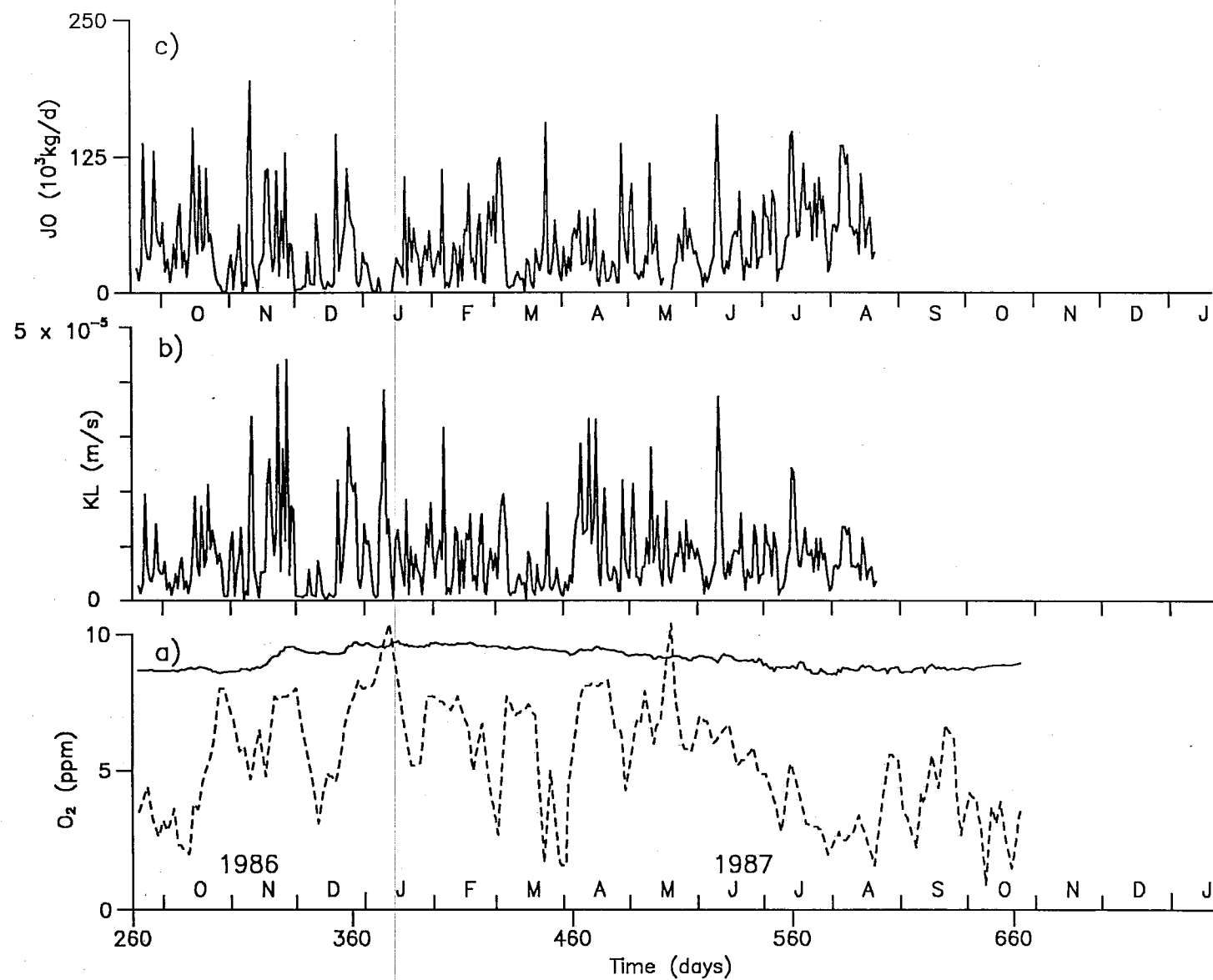
Figure 13.  Time series plot of a) DO concentration in the bulk of the fluid and the saturation value, b) the transfer velocity, KL, and c) the aeration rate.

$$Y = 1/(1 - e^{K.5}) * KT^2/(KT + 1)$$

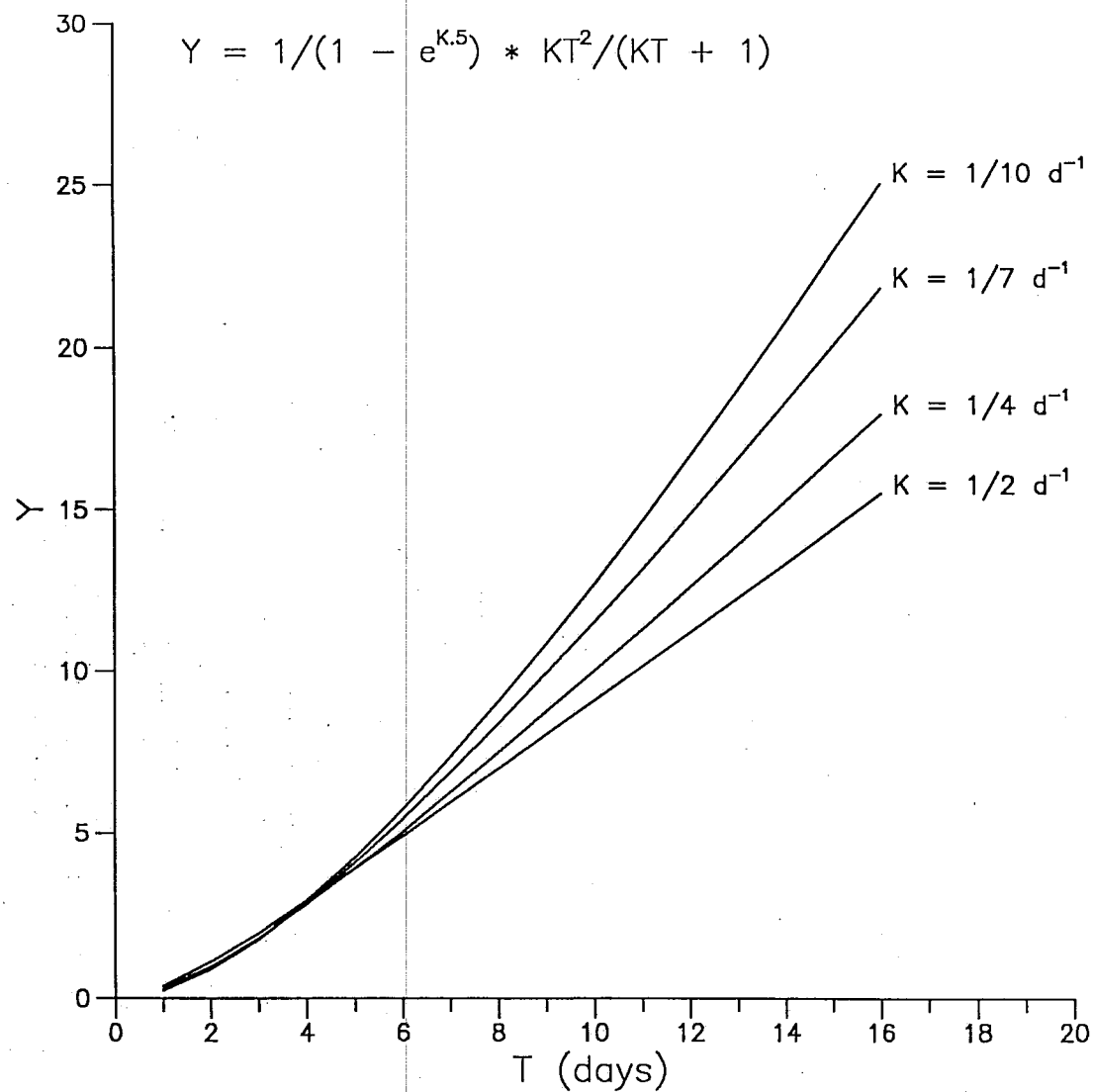K = 1/10 d⁻¹

K = 1/7 d⁻¹

K = 1/4 d⁻¹

K = 1/2 d⁻¹

Figure 14. The plot of the dependance of oxygen deficit on the reaction constants and flushing times.